To the Graduate Council:

I am submitting herewith a thesis written by Charles Lanier Britton, Jr. entitled "A Negative-Curvature Nuclear Pulse Filter." I recommend that it be accepted in partial fulfillment of the requirements for the degree of Master of Science, with a major in Electrical Engineering.

J. Frank Pierce

J. Frank Pierce, Major Professor

We have read this thesis and recommend its acceptance:

Walter L. Green

T. Vaughn Blalock

Accepted for the Council:

L. Evans Roth

Vice Chancellor
Graduate Studies and Research

A NEGATIVE-CURVATURE NUCLEAR PULSE FILTER

A Thesis

Presented for the

Master of Science

Degree

The University of Tennessee, Knoxville

Charles Lanier Britton, Jr.

June 1978

ACKNOWLEDGMENTS

The author would like to express his thanks to the many people who gave assistance in the preparation of this thesis. First of all, the author would like to thank Dr. Neven Karlovac and ORTEC, Inc. without whose support this thesis would not have been possible. Those at ORTEC who helped were Tom Becker, Terry Mayhugh, and Dr. T. J. Paulus. Gratitude is also expressed to the Hewlett-Packard Co. and Dr. Joe Millard, Van Harrison, Dave Granteer, Cyril Smith, and Don Zimmer. Thanks are also expressed to Gina Anderson for the figures, and Chris Barr and Naudell White for typing. Finally, gratitude is expressed to the thesis committee of Drs. J. F. Pierce, T. V. Blalock, and Walter Green, and the author's parents Mr. and Mrs. C. L. Britton.

ABSTRACT

A set of nuclear pulse filters developed by C. H. Nowlin has complex and real poles lying on a straignt line of constant σ. Two of these filters, one having five poles and one having seven poles, have very desirable noise and pile-up characteristics. This study considers a variation of the above filters in which the poles are located on a line having a negative curvature rather than on a straight line.

This study includes a theoretical analysis of both the noise and the pile-up characteristics of both types of filters. Using one five-pole filter of each type, the cusp factors for the two filters were calculated and found to be approximately equal to 1.13. The pile-up characteristics of the filter having poles on a negative curvature appeared to be better than that of the filter having poles lying on a straight line. Equating the noise performance for two five-pole filters, the ratio of the peak shift at high count rate was approximately 1.8 and the ratio of the peak spreading was 1.8.

Although these results were not verified experimentally, pulse-shaping filters with poles lying on a line having a negative curvature may be superior at high count rates to comparable filters having poles lying on a straignt line of constant σ.

TABLE OF CONTENTS

LIST OF FIGURES

CHAPTER I

INTRODUCTION

In recent years, the use of semi-Gaussian shaping has increased to the point where most nuclear pulse height analysis employs semi-Gaussian shaping for the filtering. This widespread use is due partly to the fact that semi-Gaussian shaping can be realized relatively easily with excellent results. One of the best published sets of semi-Gaussian filters is one by C. H. Nowlin.[1] One of his filters employs seven line poles and two complex zeros in the complex plane. Another uses five line poles and two complex zeros. Complex poles were used because fewer complex poles are needed to achieve the same apparent number of integrations than real poles.

Nowlin's paper did not present the time response at very low voltage levels of the Gaussian signal of either filter studied in this thesis. He indicated some further development in the direction of a negative curvature of poles rather than the straight-line configuration which he used.

The objective of this thesis is to investigate, as suggested by Nowlin, a constellation of poles having a given negative curvature. Both theoretical time response and theoretical noise performance will be investigated. The time response investigation will employ the Continuous Systems Modeling Program (C.S.M.P.) to simulate the impulse response of the filter. The frequency of poles and zeros of the transfer function will be adjusted in discreet increments with the objective of studying the time response. The noise characteristics of the optimized filter will then be investigated using a parameter known as the cusp factor. The cusp factor is the ratio of the noise-to-signal ratio of a shaping filter and the noise-to-signal ratio of the ideal cusp. All indicators of performance will then be examined together in order to obtain the most useful pole-zero constellations.

Chapter II is concerned with the requirements and limitations encountered in nuclear pulse spectroscopy. The ideal cusp is defined in the time domain. Various methods of pulse shaping are then discussed. The discussions include the various means of implementation and the shortcomings encountered with the individual methods.

Chapter III describes the requirements of a nuclear pulse filter including noise and time response. In particular, the chapter is concerned with semi-Gaussian shaping and the particular characteristics associated with this type of shaping. The discussion includes an explanation of the use of complex poles and zeros.

Chapter IV is a presentation of the time- and frequency-domain characteristics of the filters being considered. The impulse responses of the filters are derived from the Laplace transform representations. A computer simulation program is used to generate plots of the filter impulse responses. The plots are then compared with respect to pulse symmetry.

Chapter V presents the method and results of the time-response study of the filter. The study is in essence a sensitivity study of the basic filter developed by the author. The parameter studied is that of the sensitivity of the shape factor S to the pole or zero positions. These data are plotted graphically.

Chapter VI is a summary of the noise performance of the filters and the criteria used to measure the performance. The main performance criteria, the cusp factor, is developed for a general class of filters. The cusp factor is then calculated for the optimized filter cases of Chapter V.

Chapter VII then takes the C. B. 1 filter and calculates an estimation of pile-up distortion for the filter. An estimation is also calculated for the N = 5 filter. The pile-up effects are compared with optimum cusp factors and then with equal cusp factors. Conclusions are then reached about which filter would be most useful in a spectroscopy system.

Chapter VIII is a general summary of the thesis. This chapter includes the findings of the previous chapters and suggestions for further study.

CHAPTER II

NUCLEAR PULSE SPECTROSCOPY

A nuclear spectroscopy system has three fundamental blocks; signal source, signal processing, and information storage. The first two, signal source and signal processing, are the only two functional blocks considered here. The information with which this thesis is concerned is the peak height of a pulse from a nuclear pulse amplifier. This peak height is proportional to the energy of certain radiated particles. This thesis is concerned with the transfer function of such a nuclear shaping amplifier.

The signal source of a nuclear spectroscopy system is called a detector. There are many different kinds of detectors. The only kinds which will be considered here are solid state detectors which have very high resolution. These detectors emit a quantity of charge proportional to the energy lost by a particle travelling through the detector. The charge emitted ranges from a few hundred to a few million electrons. Since this quantity of electrons is so small, the signal must be amplified to be usable. Along with this amplification comes the problem of noise. Any noise that is introduced with the signal will be amplified along with the signal. Therefore, a low-noise amplifier must be used to amplify this charge. An integrator is usually chosen for this because it has a low-noise configuration. This integrator has a very high charge gain and is called a charge-sensitive preamplifier. For a quantity of charge collected by the integrator, the output signal is shown in Figure 2-1. This output is useful in that its peak height is proportional to the amount of charge collected from the detector. The tail is, however, long in time with respect to the usual average rate of pulses. A desirable alternative is to shorten the pulse while retaining its vital characteristics such as peak height and low noise.

The pulses being considered have a random time distribution. They also exhibit an average rate. The pulses tend to pile up on each other due to the length of the tails of the pulses. This pile-up causes the peak voltage value to shift from its true value. This shift causes inaccuracies in the measurements. The narrower the pulse, the less chance there is of this pile-up occurring. Narrowing the pulse, however, presents a problem in that a narrow pulse will contain more noise since the bandpass required for a narrow pulse is wider than for a longer pulse. A compromise must be reached between a narrow pulse and a low-noise pulse. A nuclear shaping amplifier is used to provide the transfer function for such a pulse. Properly used, the amplifier will improve the noise performance of a nuclear pulse system and will also allow high counting rates to be used.

The optimum pulse as far as noise is concerned is called the ideal cusp.[2] The ideal cusp is the pulse which will give optimum performance with respect to noise when considering a standard nuclear pulse shaping system. The details of the noise spectrum considered will be covered in Chapter VI. The ideal cusp has the impulse response given by

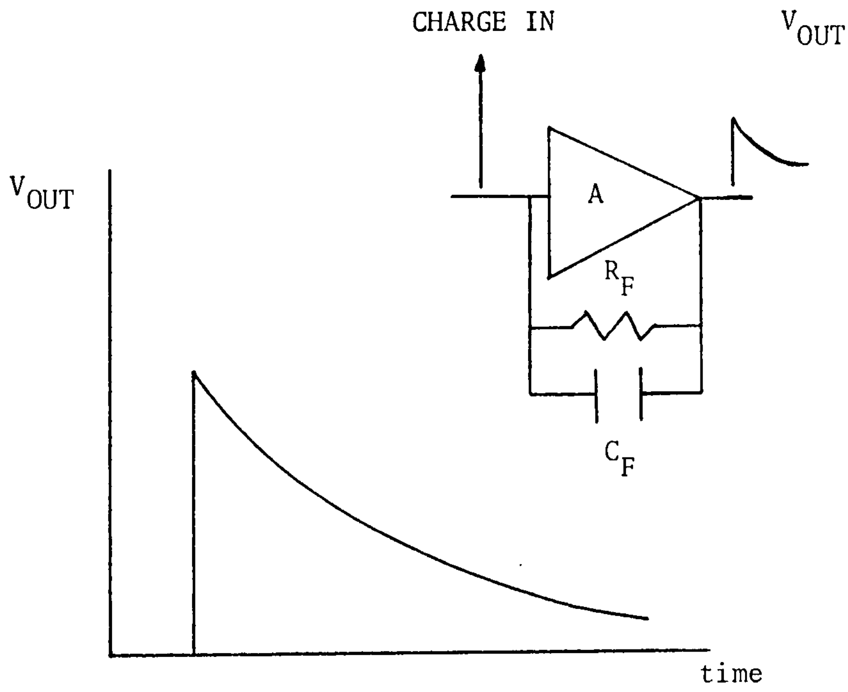

Figure 2-1. Charge Sensitive Preamplifier.

$$h(t) = e^{-\alpha|t|} \quad , \; -\infty < t < \infty \qquad (2\text{-}1)$$

where α is the noise corner frequency. The noise corner frequency will be discussed in detail in Chapter VI.

Obviously, the ideal cusp is not physically realizable due to the fact that the cusp is a noncausal response. If the pulse could in fact be realized, the infinite "tails" of the pulse would cause peak shifting due to pulse pile-up.

Several different methods of pulse shaping have been developed over the past several years.[3] Each method has certain drawbacks. All of the methods fall short of the noise performance of the ideal cusp. The following methods are those that have proven most useful in a variety of applications.

I. CR-RC SHAPING

CR-RC shaping involves differentiating the input signal with respect to time in order to shorten the length of the pulse. As previously mentioned, this shortening of the pulse produces a reduction in the "piling-up" effect. The differentiated pulse is then integrated. This integration serves a multifold purpose. One purpose is to reduce the amount of noise present in the output signal by reducing the available bandpass in which noise can be present. Another purpose of the integration is to reduce ballistic deficit. Ballistic deficit is the sensitivity of the peak value of a particular pulse to risetime variations of an incoming signal. As the risetime of the input signal is increased, the peak height of the differentiated signal decreases. If an integrator follows the differentiation, variations of risetime at much higher frequencies than the integrator will be less noticeable.

CR-RC shaping is illustrated in Figure 2-2. The signal at the output of the Charge-Sensitive Preamplifier (CSP) has the form

$$\frac{V_{IN_D}}{V_{IN}} = \frac{1}{sC_F} \tag{2-2}$$

where C_F is the feedback capacitor. Equation (2-2) is only approximate since the feedback resistor R_F has some finite resistance and the amplifier A has limited gain.

If the CSP has zero output impedance and A_1 has infinite input impedance, $\frac{V_{O_D}}{V_{IN_D}}$ can be written as

$$\frac{V_{O_D}}{V_{IN_D}} = \frac{R_D}{\frac{1}{sC_D} + R_D} \tag{2-3}$$

Multiplying numerator and denominator by sC_D, we have

$$\frac{V_{O_D}}{V_{IN_D}} = \frac{sC_DR_D}{1 + sC_DR_D} \tag{2-4}$$

Letting $C_DR_D = \tau_D$, the final form for the differentiator is

$$\frac{V_{O_D}}{V_{IN_D}} = \frac{s\tau_D}{1 + s\tau_D} \tag{2-5}$$

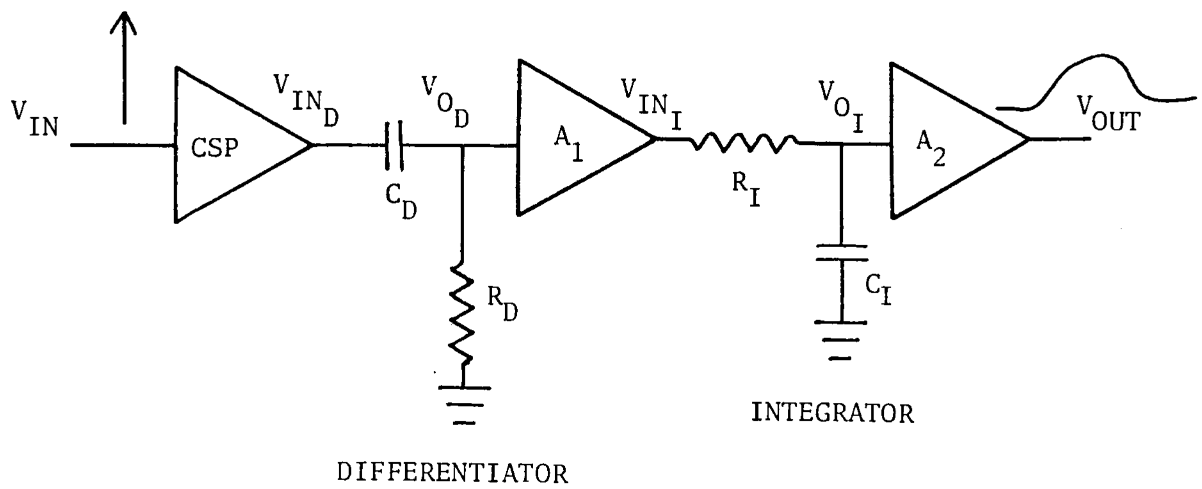

Figure 2-2. CR-RC Shaping.

Assuming A_1 has zero output impedance

$$\frac{V_{O_I}}{V_{IN_I}} = \frac{\frac{1}{sC_I}}{R_I + \frac{1}{sC_I}} \tag{2-6}$$

Multiplying numerator and denominator by sC_1, we obtain

$$\frac{V_{O_I}}{V_{IN_I}} = \frac{1}{1 + sC_I R_I} \tag{2-7}$$

Letting $\tau_I = C_I R_I$ the final form for the integrator is

$$\frac{V_{O_I}}{V_{IN_I}} = \frac{1}{1 + s\tau_I} \tag{2-8}$$

The complete transfer function for the shaping network is

$$\frac{V_{OUT}}{V_{IN}} = \frac{A_1 A_2 s\tau_D}{sC_F(1+s\tau_D)(1+s\tau_I)} \tag{2-9}$$

Nicholson stated that if $\tau_D = \tau_I$, the best compromise between a flat pulse top for low ballistic deficit and a quick return to zero volts for low pile up is obtained. He also stated that this condition of $\tau_D = \tau_I$ gives the highest signal-to-noise ratio. Because of these three findings, the values of τ_D and τ_I are normally made equal.

II. SINGLE DELAY-LINE SHAPING

Suppose a delay line is shorted at one end. A delay line whose transmitting end is properly terminated in the characteristic impedance of the line and whose receiving end is shorted will have a single reflection at the receiving end. This reflection will be an inversion of the original signal. When this reflected, inverted signal returns to the transmitting end of the line, the reflected signal will sum with any signal that is still present at the transmitting end. This reflection effect is the basis for single delay-line shaping illustrated in Figure 2-3. The transmitting end of the delay line is terminated and connected to the output of a CSP. As the approximate step output of the CSP is delayed, inverted, and summed with itself, and output signal is obtained as in Figure 2-3. This flat-topped pulse would seem to be ideal as far as ballistic deficit and pile up are concerned. A drastic increase in risetime would be needed to affect the peak height noticeably. The pulse width is controlled by the delay time of the line. If T_D is the desired pulse width, the delay time of the line should be $T_D/2$. The problems associated with the line are due to the fact that the delay lines have parasitic components associated with them which distort the signal as it travels down the line. The line also attenuates the signal which prevents complete cancellation. Also, due to the fact that the line theoretically has no frequency limitations, the only signals that can be usefully processed are those whose signal peaks are greater than that of the noise. Normally the limiting frequency of amplifiers

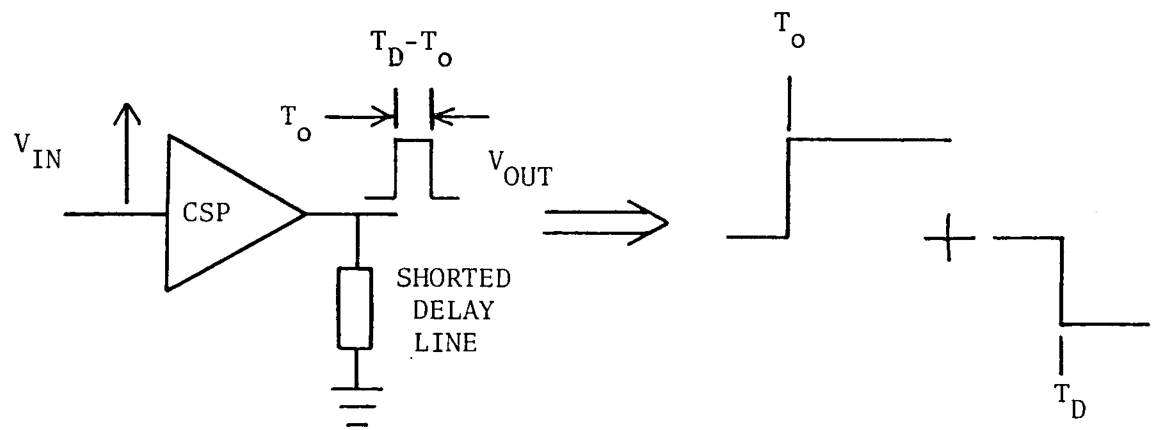

Figure 2-3. DL Shaping.

following the line will limit the noise somewhat, or a pole can be intentionally added to reduce the noise, as is often the case. Other methods may be used to achieve single delay-line shaping. Usually these other ways improve on the simple method presented here.

III. DOUBLE DELAY-LINE SHAPING (DL)[2]

Double delay line shaping is similar to delay line shaping except that another delay line is added after the first line which is identical to the first line. The second line adds a negative lobe to the first pulse resulting in a bipolar pulse. The bipolar pulse can be fed through an integrator resulting in a triangular shaped pulse. The triangular pulse is a close approximation to the ideal cusp as far as signal-to-noise ratio is concerned. The triangular pulse also returns quickly to the baseline. Unfortunately, a true integration is difficult to realize so that a triangular pulse cannot be exactly realized. The single delay line is often used to approximate the triangular pulse by passing a single delay line pulse through a low-frequency pole configuration. This method does not return to the baseline as quickly as the double delay-line method, but it is simpler than the double delay-line method using an integrator due to the pointed peak. Double delay-line shaping is presented in Figure 2-4.

IV. TRANSVERSAL FILTERS[4]

The theory behind the transversal filter of Figure 2-5 is straightforward. A signal is fed into a delay line which is tapped

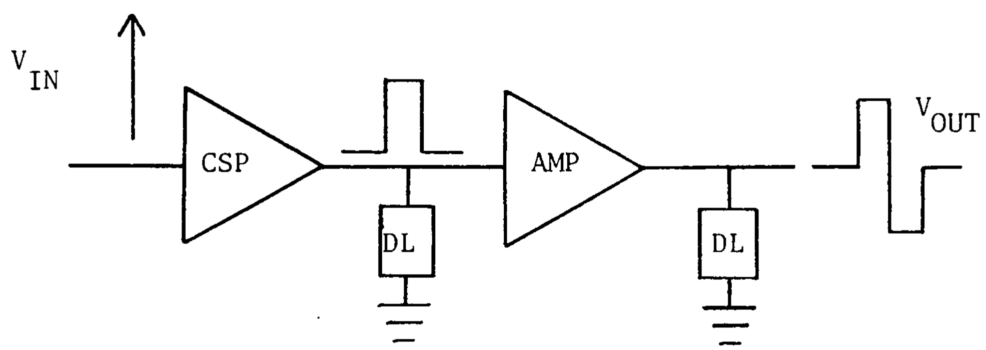

Figure 2-4. DL^2 Shaping.

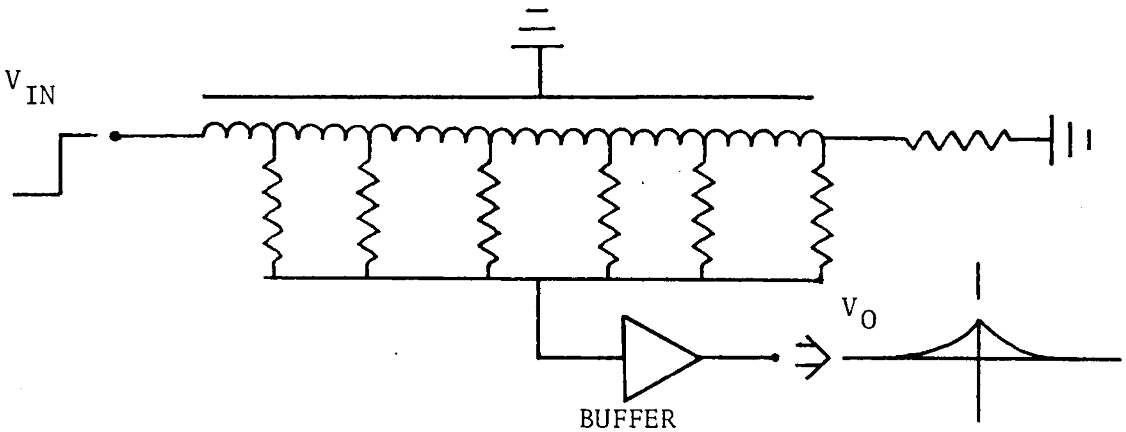

Figure 2-5. Transversal Filter.

at several points along its length. The signals taken from each of these points are weighted according to a predetermined design based on the desired output signal. The signals are weighted by varying the amplitude of each signal extracted. The weighted signals are then summed to produce an output signal. Almost any shape of output signal can be realized using this method of filtering.

Transversal filters have been in existence for many years. The idea is thought to be traceable to Nyquist in 1928. The use of this method of filtering has been limited to the fields of communications and radar primarily due to economic reasons. The recent development of analog delay lines has made the transversal filter more economical to develop and use. The analog delay line employs solid state devices to store an input signal for some period and release that signal at a later time. If all delayed outputs are properly weighted and summed, the resulting filter is of the transversal variety.

Since any shape of output signal can be produced, the transversal filter can produce the triangular pulse previously mentioned, the flat-topped unipolar pulse, or the semi-Gaussian which will be discussed next. The primary drawback to the analog delay line filter are linearity problems with the lines themselves and frequency response problems due to the limited rate at which charge in the devices can be shifted.

V. SEMI-GAUSSIAN SHAPING[5]

Semi-Gaussian shaping, Figure 2-6, is presently the most widely used method of pulse shaping. Semi-Gaussian shaping is used because

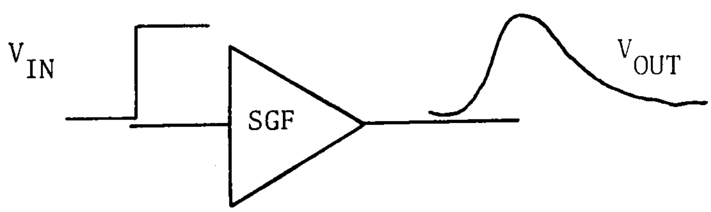

Figure 2-6. Semi-Gaussian Filter.

a true Gaussian pulse shape has a signal-to-noise ratio close to that of the ideal cusp. Also, the Gaussian pulse has a rounded top so that the effect of ballistic deficit would not be as noticeable as the effect on the infinite cusp. The Gaussian waveform is not in itself useful, however, because of the very nature of the time response. The waveform itself takes an infinite amount of time to be complete. Semi-Gaussian shaping is useful because it is realizable and retains many of the useful properties of Gaussian shaping.

Semi-Gaussian shaping is realized theoretically by employing a single CR differentiation and an infinite number of integrations, all with equal RC time constants as in CR-RC shaping. A practical realization is that of a single CR differentiation and four RC integrations. Other practical realizations are those of the filters presented in this thesis. The tail of the semi-Gaussian pulse does not return to the baseline as quickly as the tail of the double delay-line pulse with an integrator. Pile up errors are caused by this slow return to the baseline.

VI. SUMMARY OF SHAPING METHODS

Of the various methods of pulse shaping, the most promising in a long term sense appears to be the transversal filter. Almost any pulse shape can be realized using this method. The hardware necessary for such a filter is still more difficult to use than that of the other methods. The delay-line methods are excellent, as far as noise is concerned. Their main drawbacks are uncertainties in the lines themselves and ballistic deficit due to the pointed peak. Simple CR-RC shaping is a very simple, straightforward method of shaping. The tail of the pulse is too long for the method to be useful at high count rates. True Gaussian and the ideal cusp are both useful as low-noise peaks but are physically unrealizable. Alternatively, the most useful in terms of noise performance, count rate performance and ease of realization is semi-Gaussian shaping. This thesis will be concerned solely with this method of shaping. A comparison of the various methods[6,7] thus far discussed with respect to noise is presented in Table 2-1. Included in this table is the performance of the five- and seven-pole filters developed by Nowlin.

TABLE 2-1

NOISE COMPARISON

Type of Filter	Relative Noise-To-Signal Ratio
Cusp (reference)	1.000
$(DL)^2$ integrated triangle	1.075
DL + RC low-pass filter	1.098
True Gaussian	1.120
Nowlin's N = 5 semi-Gaussian	1.131
Nowlin's N = 7	1.135
CR-RC	1.359

CHAPTER III

SELECTION OF POLE-ZERO CONSTELLATION

The selection of a proper pole-zero constellation in a semi-Gaussian filter is of utmost importance in nuclear pulse shaping. The pole-zero constellation is the heart of any signal processing system. The constellation must meet several requirements. The first requirement is that the constellation must have a high signal-to-noise ratio. This requirement is necessary so that the signal peak can be determined with a high degree of accuracy in the presence of noise. The second requirement is that the signal be of short duration. The reason for this has already been stated in that at high counting rates, pulses will tend to "pile up" on each other and cause a shift in the peak height. A third requirement is that the pulse shape be relatively insensitive to pole position variations. This requirement is necessary due to the fact that physical realizations of filters must use components which typically have tolerances on the values. These tolerances could greatly affect transfer functions whose sensitivity to component variations is high.

The particular method of pulse shaping studied in this thesis is semi-Gaussian. Semi-Gaussian shaping is used due to the fact that the semi-Gaussian pulse shapes of Nowlin's five- and seven-pole filters have a noise performance only 13% worse than that of the ideal cusp. The semi-Gaussian is also much less sensitive[8] to input risetime than are the delay line pointed top pulses. This good ballistic deficit performance is important when working with a variety of charge sensitive preamplifiers (CSP) each having a different risetime. The semi-Gaussian pulse is especially well adapted to a system which necessitates the use of several peaking times of the output waveform. Different detectors require different bandpass filters due to the power spectral density of the noise of the individual detector preamp system. The criteria for selecting the proper frequency of the bandpass will be covered in Chapter VI.

In this thesis the only pulse type considered will be the semi-Gaussian unipolar pulse. The unipolar means that the pulse is always above the baseline of zero volts. Another type of pulse used in spectroscopy is called the bipolar pulse. The bipolar pulse exists both above and below the baseline. The bipolar pulse obtained from a semi-Gaussian pulse is simply a semi-Gaussian pulse which has been differentiated.[9] This particular type of pulse is useful in very high counting rate systems. If the ideal semi-Gaussian pulse is differentiated the area in the upper lobe of the pulse will equal the area in the bottom lobe of the pulse. Because of this fact, the baseline would be less subject to shift at high count rates. This equal area pulse is useful in A. C. coupled systems. If a unipolar pulse was used in an A. C. coupled system the baseline would shift as count rate increased. The noise performance of the double differentiated pulse is worse than that of the unipolar pulse. The unipolar pulse is therefore the pulse which is used most widely. When used properly in a spectroscopy system, the unipolar pulse will exhibit excellent performance.

Complex poles are used in the amplifiers presented in the thesis because fewer complex poles are needed to achieve the same apparent number of integrations than real poles. This property of complex poles is useful when realizing a filter with actual components because of the simplification in circuitry.

Complex poles present other problems however. The impulse response of a complex pole pair is a damped sinusoid. This sinusoid of course has an infinite number of local maxima or minima, or excess peaks as they will be called, which are not desirable. The only peak which is desirable is the first maximum. This peak holds the desired amplitude information. The excess peaks could show up as peak shift if the main peak of a pulse occurred at the same time as an excess peak from a previous pulse. The excess peaks themselves could appear as separate events on a nuclear pulse height analyzer if the peaks were in the neighborhood of 50 mV or greater.

The standard complex filter constellations, i.e., Butterworth, Bessel, etc., have desirable time-domain characteristics except for the predominance of large amplitude excess peaks in the impulse response. These excess peaks are very undesirable as has already been stated. These pole constellations have a positive radius with respect to the origin in the s-plane; i.e., the outermost poles are closer to the $j\omega$ axis than the innermost poles (those closest to the σ axis).

In particular, the Butterworth standard low-pass forms consist of a semicircle centered at the origin of the s-plane along which the poles lie. This semicircle extends into the left-half plane. These forms can be seen in Figure 3-1.[11] The impulse response for an n = 4 Butterworth filter has approximately 18% undershoot. Obviously 18% undershoot is strictly unusable.

The Bessel low-pass filters are similar to the Butterworth filters except that the Bessel filters lie on eccentric circles extending into the left half plane with centers on the σ axis in the right half plane. The Bessel filters also have undershoot; not as much, however as the Butterworth.

The pole-zero constellation must be chosen in such a way as to minimize these excess peaks. Nowlin's filters employ complex and real poles on a line of constant σ; i.e., constant real part. The poles he uses have equal spacing along the $j\omega$ axis or imaginary axis. Nowlin suggested that other constellations could be used. He suggested that a constellation employing a negative curvature of poles would have very low amplitude excess peaks also. This suggestion is the basis for this thesis. A negative curvature filter was developed and named the C. B. 1. The C. B. 1 pole-zero constellation was discovered during an experimental evaluation of nuclear pulse filters. The pole-zero constellation of the C. B. 1 as well as Nowlin's five and seven pole filters can be seen in Chapter IV. None of these filters have any visible excess peaks above 10^{-4} of the peak value of the impulse response.

Complex zeros have been added to the pole constellations. These zeros tend to lengthen the leading edge of the impulse response, thus increasing the symmetry. Symmetry is a property which will be examined in the impulse response portion of this thesis. The ideal Gaussian

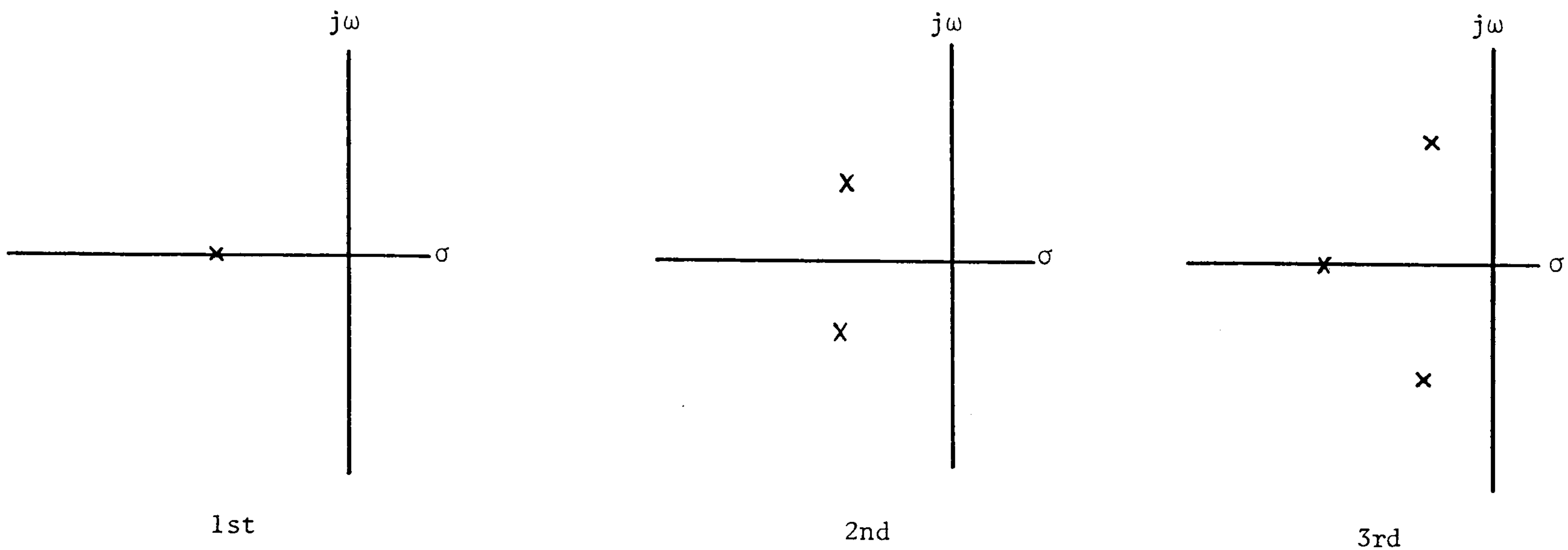

Figure 3-1. First, Second, and Third Order Butterworth Forms.

waveform is perfectly symmetrical about the peak. The C. B. 1 filter employs zeros to increase the symmetry about the peak.

The zeros are also useful in the frequency domain response of the filter. Complex zeros with no real part in their Laplace transforms are actually notch filters. These notches in effect "remove" area from underneath the frequency versus amplitude curve. Removing area from underneath the curve removes available passband through which noise can be processed. The noise will then be lowered overall. A problem occurs if the notch also falls on an important harmonic of the signal itself. The signal amplitude could be decreased more than the corresponding noise decrease thus worsening the overall noise performance.

In summary, this chapter has discussed the inadequacy of standard Butterworth and Bessel filters with respect to time-response requirements imposed by nuclear pulse systems. A new pole-zero constellation discussed by Charles Nowlin was suggested. Nowlin's filters tend to suppress the excess peaks exhibited by complex poles. Nowlin also suggested using a negative curvature version of his filters. The negative curvature filter will be studied and developed in this thesis.

CHAPTER IV

FREQUENCY- AND TIME-DOMAIN CHARACTERISTICS

This chapter will deal with the frequency-domain and time-domain characteristics of Nowlin's five pole and seven pole filters, and the C. B. 1 filter. The Laplace transform representation of all three filters will be presented. The impulse response of each of the three filters will be derived from each filter's respective Laplace transform. A comparison between the three filters concerning the symmetry of the pulses will then be presented using a computer simulation program. The results from the comparison will be discussed.

I. LAPLACE TRANSFORM REPRESENTATIONS

The Laplace transform representations are presented in Figures 4-1, 4-2, 4-3. Both of Nowlin's filters are, as previously explained, straight line constellations of poles. The $N = 5$ constellation of Nowlin has, for a σ equal to one for the line poles, a Q equal to 0.9 where Q equals the ratio of the complex part of the innermost complex pole to the real part of the complex pole. The $N = 7$ constellation has a Q equal to 0.6. The C. B. 1 is a negative-curvature of poles. The Q does not apply to the C. B. 1 since the C. B. 1 is not a straight line of poles. The Q was used by Nowlin to determine the magnitude of the excess peaks in the straight line constellation without zeros. Nowlin's $N = 7$ constellation and the C. B. 1 constellation are given

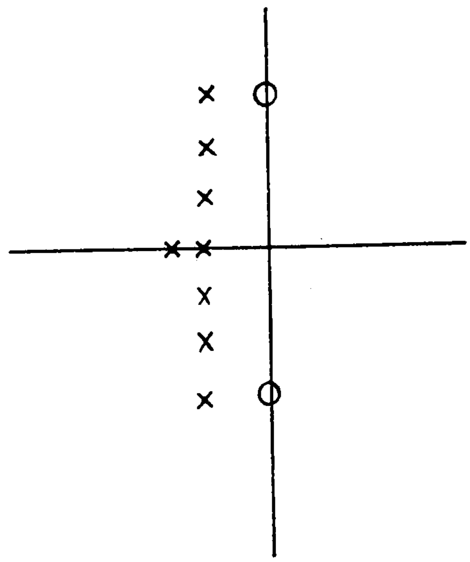

Figure 4-1. Nowlin N = 7 Form.

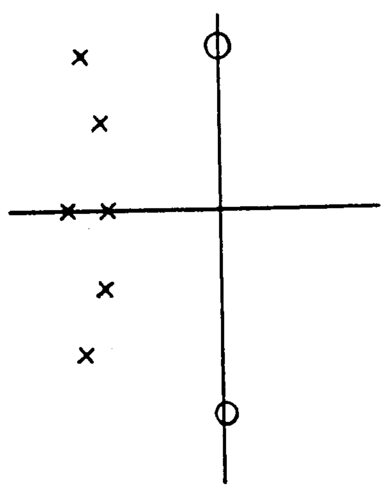

Figure 4-2. C. B. 1 Form.

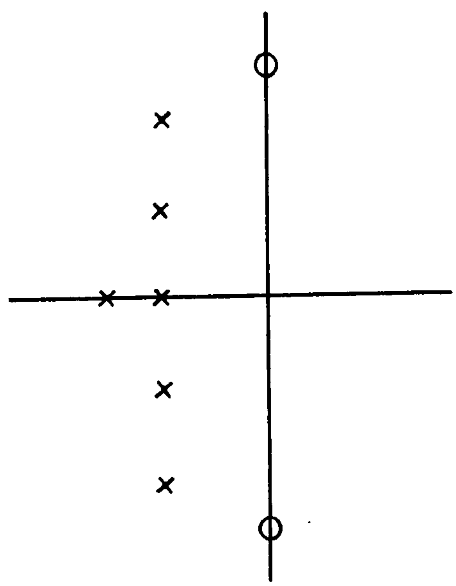

Figure 4-3. Nowlin N = 5 Form.

for peaking times of 4.32 sec. and 4.03 sec. respectively while Nowlin's N = 5 constellation is given for a peaking time of 3.49 sec. The Laplace transforms are, for Nowlin's N = 5 filter

$$H(s) = \frac{s^2 + 4.0501}{(s+1.4)(s+.875)(s^2+1.75\ s+1.3858)(s^2+1.75s+3.2462)} \quad (4.1)$$

for Nowlin's N = 7 filter

$$H(s) = \frac{s^2 + 3.24}{(s+1)(s+1.5)(s^2+2s+1.36)(s^2+2s+2.44)(s^2+2s+4.24)} \quad (4.2)$$

and for the C. B. 1

$$H(s) = \frac{s^2 + 2.4797}{(s+.85663)(s+1.4782)(s^2+1.803s+2.162)(s^2+1.75s+1.187)} \quad (4.3)$$

Truncation and rounding were used on the coefficients.

II. FILTER IMPULSE RESPONSES

The impulse responses of the filters were obtained through inverse Laplace transform methods from the Laplace transforms. These equations were used as a monitor on the computer accuracy presented in the next subsection. The method used for these transforms was that of partial fraction separation followed by an inverse Laplace transform. The final equation obtained for Nowlin's N = 7 is

$$h(t) = -3.0518e^{-1.5t}+e^{-t}[5.04877-(1.78013)(\cos(0.6t)+2.4 \sin(0.6t) -(0.312837)(\cos(1.2t)-3.08108 \sin(1.2t))+(0.102015)(\cos(1.8t) -0.6020076 \sin(1.8t))] \quad (4.4)$$

for Nowlin's N = 5 filter

$$h(t) = -4.63644e^{-1.4t}+e^{-0.875t}[5.96231-1.08106(\cos(0.7875t) +3.60456 \sin(0.7875t))-0.2449(\cos(1.575t) -1.6451 \sin(1.575t))] \quad (4.5)$$

and for the C. B. 1

$$h(t) = 9.07237e^{-0.85663t}-5.68259e^{-1.4782t} -2.60061e^{-0.875t}[\cos(0.64913t)+3.22045 \sin(0.64913t)] -0.78818e^{-0.9015t}[\cos(1.161t9t)-1.98860 \sin(1.16159t)] \quad (4.6)$$

These impulse responses are made up of a damped summation of sinusoids summed with an exponential. All three responses are monotonically increasing before the peak and monotonically decreasing after the peak. Monotonicity is one of the main requirements for a filter used in pulse shaping.

III. COMPUTER SIMULATION

The three impulse responses were simulated by using the Continuous Systems Modeling Program (CSMP). This program is a digital computer program which converts a Laplace transform into an impulse response.

A plot of amplitude versus time was obtained for each impulse response. The programs used are presented in Appendix A.

The parameter of interest that was calculated from the time versus amplitude plot is the shape factor S.[12] The shape factor is defined as

$$S_{0.1\%} = \frac{\tau_{0.1\%} + \tau_p}{\tau_p} \tag{4.7}$$

where $\tau_{0.1\%}$ is equal to the maximum time between crossings of 0.1% of the peak value and τ_p is equal to the time between the first 0.1% crossing and the peak. For a perfect semi-Gaussian pulse, S should have a value of 2. The $S_{0.1\%}$ values for the three amplifiers are presented in Table 4-1. The $S_{0.1\%}$ for the N = 7 filter is 3.58% better than the C. B. 1. The $S_{0.1\%}$ for Nowlin's N = 5 is 24.45% worse than the C. B. 1.

The S value for a filter is a measure of the symmetry of the impulse response of that filter. Two filters that have equal peaking times and unequal values of S will not perform the same at high count rates. The amplifier with an S value closest to 2 will perform better in the count rate region where the resolution is limited by pulse pile-up and not by noise. This statement assumes that the two filters have similar noise characteristics. At very low count rates where resolution is limited by noise, the shape of the pulse has very little effect on the resolution. If two filters have different peaking times but similar noise characteristics, the filter that returns more quickly to

TABLE 4-1

0.1% S VALUES

Filter	0.1% S Value
N = 7	2.69
N = 5	3.50
C. B. 1	2.79

the baseline will have a better high count rate resolution. In this case S is meaningless as far as performance is concerned.

The value of 0.1% is an arbitrary level of reference. The 0.1% level is an easy value to obtain for a 10V peak pulse. The 0.1% level would be the 10mV level of the pulse and this level could be visually determined quite easily using a standard laboratory oscilloscope.

The total pulse length will be the determining factor for the high count rate performance of the filters. Optimum noise performance determines the peaking time of a filter. The S value is a comparative factor for symmetry only. Figure 4-4 shows the three different pulse responses. The peaking times and pulse heights are normalized for comparison.

The factor S will be used in the next chapter to study the symmetry of the pulse. The C. B. 1 is not as symmetrical as is possible. S will be used as the factor to be studied. Since S is not useful by itself, other parameters will be considered in Chapter VI.

In this chapter the Laplace transforms and impulse responses of the three filters being studied have been presented. The shape factor S has been defined as a parameter which gives an indication of the symmetry of a semi-Gaussian waveform. The factor S is a comparative factor only in the sense that other information must be obtained for S to be useful.

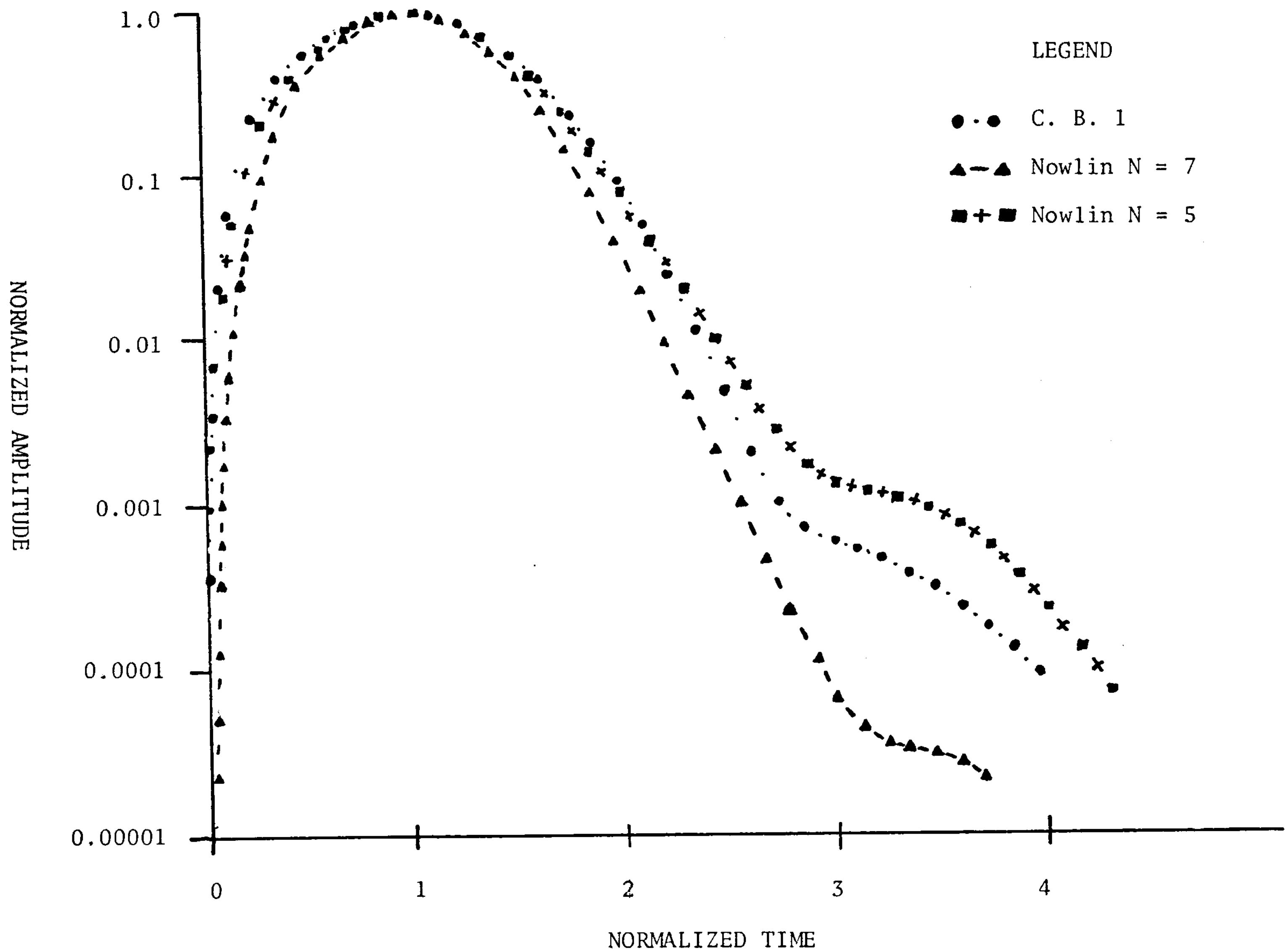

Figure 4-4. Computer Simulation.

CHAPTER V

FILTER TIME-RESPONSE STUDY

This chapter will present the time-response study of the pole-zero constellation of the C. B. 1 filter. The data will be in the form of a sensitivity study. The sensitivity of the shape factor S to changes in the individual pole or zero movements will be calculated. Those cases in which the shape factor is improved will be examined for quality of noise performance in Chapter VI. The filter whose overall symmetry and noise performance is most desirable will be compared directly with Nowlin's N = 5 filter in Chapter VI.

A true optimization program for a filter such as the C. B. 1 would surely be prohibitively complex. Each set of poles would be allowed to wander in the s-plane with respect to the other poles in any direction. Nowlin's time-response study would have much more limitation due to the unchanging relative position of the line poles. This is because Nowlin's filters have a particular locus for the line-poles, i.e., all the poles fall on a straight line except for one. The C. B. 1 has no such locus. Because of this, the time-response study of the C. B. 1 will vary each set of complex poles in both the σ and $j\omega$ direction.

The sensitivity of the shape factor was chosen as the variable to be examined for two reasons. First, the shape factor allows the user to be aware of the variation in symmetry of the output pulse due to pole or zero movement. Second, the shape factor allows the user to be aware of baseline ringing or generation of excess peaks. No other single variable gives as much useful information as does the shape factor. Furthermore, for small changes in pole-zero values, the peaking time changes very little. The length of the baseline is therefore effectively being monitored. Because of the usefulness of this variable in time-response calculations, the shape factor sensitivity was calculated.

Sensitivity is denoted by the symbol S.[13] A superscript is added to the symbol S to denote the parameter that is changing. A subscript is used to denote the parameter or element that is causing the change. The sensitivity of a filter parameter X with respect to a parameter Y is defined as

$$S_Y^X = \frac{d(X)/X}{d(Y)/Y} = \frac{d(X)}{d(Y)}\,\frac{Y}{X} \qquad (5\text{-}1)$$

Sensitivity functions are good only for infinitesimal changes in parameters, according to theory. The sensitivities calculated will characterize the change in shape factor S with respect to pole or zero movement. The poles and zeros will be moved individually. This individual movement will be used because there are an infinite number of combinations of pole and zero positions. In order to limit the scope of this thesis to a reasonable number of cases, the individual pole or zero movement will be used.

An examination of Equation (5-1) reveals that the sensitivity of X to a change in Y is equal to zero when dX/X is equal to zero.

Two modifications will be made to Equation (5-1) in this thesis. The first modification is that $\frac{Y}{X}$ will be normalized to 1. This modification will allow a direct correlation of Equation (5-1) to the graphical method of plotting which will be used. The second modification is actually a qualification of the use of Equation (5-1). As previously stated, only a monotonically increasing and a monotonically decreasing function is useful in pulse shaping. Any ringing on the baseline is therefore undesirable. Some pole movements reach a point where further movement causes the waveform to exhibit ringing on the baseline. In such a case, the sensitivity could not include the region of pole movement in which ringing occurs. This type of region will be illustrated on the graphs but not considered in the sensitivity.

The following graphs will be presented as shape factor versus pole or zero position (S versus ω or σ) and dS versus $d\omega$ or $d\sigma$. The quantity dS as a function of $d(\omega,\sigma)$ will be the modified sensitivity function. The pole and zero positions will be presented as percent deviation from nominal. The shape factor will be presented as the calculated value.

The first case will be that of the real pole at s = -0.8566 rad./sec. Figure 5-1 shows the value of S plotted against the value of σ. This figure shows that above approximately +1% change in the pole value, the waveform begins to exhibit some ringing about the baseline. This ringing is, of course, undesirable. The optimum value of the pole position with respect to shape factor will then

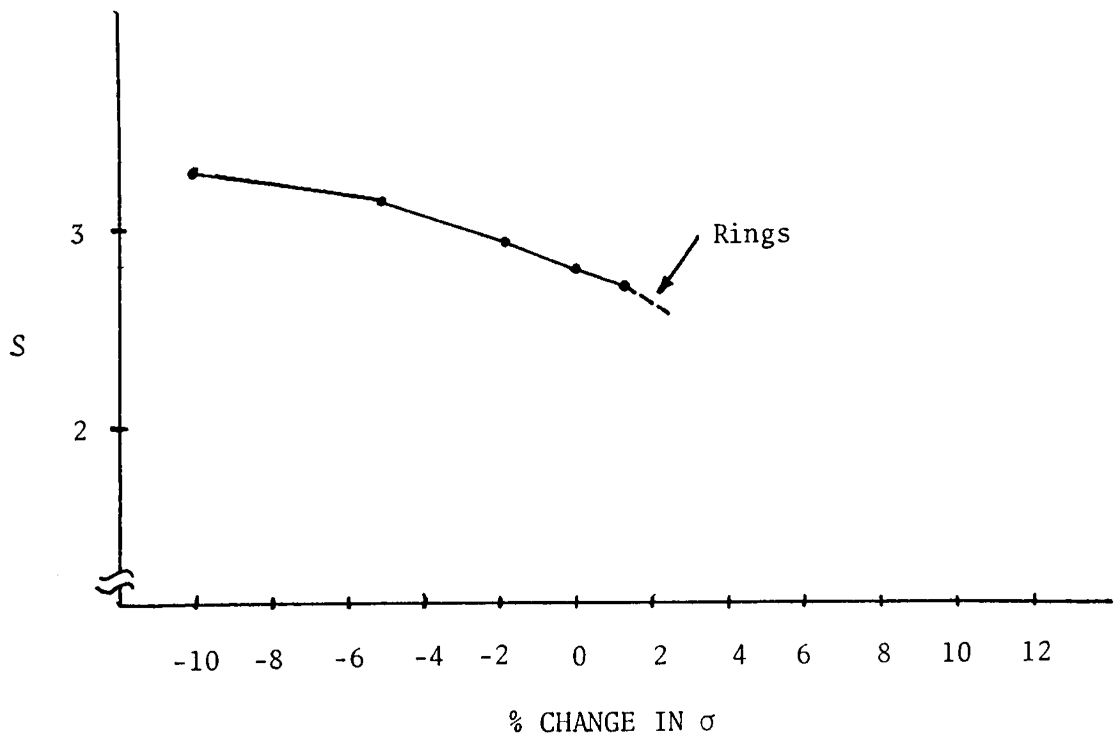

Figure 5-1. Movement of Pole at σ = -0.8566.

be approximately 1.01 times the original pole position. The sensitivity at this value is at a maximum of the values tested. Figure 5-2 illustrates this peak of sensitivity.

The values of S versus pole position for the pole at -1.47 rad./sec. are given in Figure 5-3. This outer real pole has less of an effect on the waveshape than the inner real pole at -0.8566 rad./sec. This effect is to be expected since the outer pole mainly increases the amount of damping. As this damping is removed, the waveform begins to ring about the baseline. The ringing begins to occur in the neighborhood of a +7% increase in the pole value. The sensitivity of S to the pole position is graphed in Figure 5-4. As can be seen, the optimum value of S is at a relatively low value of sensitivity. This fact makes this parameter one of the more likely parameters to adjust for good shape factor.

The values of S plotted against the position of the zeros is graphed in Figure 5-5. The zeros have a positive effect on the shape factor as they are moved inward. The visual effect on the waveform is that the leading edge of the pulse begins to exhibit a "humped" appearance as illustrated in Figure 5-6. This hump has no obvious detrimental effect on time-domain performance as long as the hump does not become a peak in itself. The hump does not become a peak until the zeros have moved in towards the origin by approximately -27%. Figure 5-7 is a graph of the sensitivity of the zero movement. The position of -27% is a more sensitive area than the original zero position.

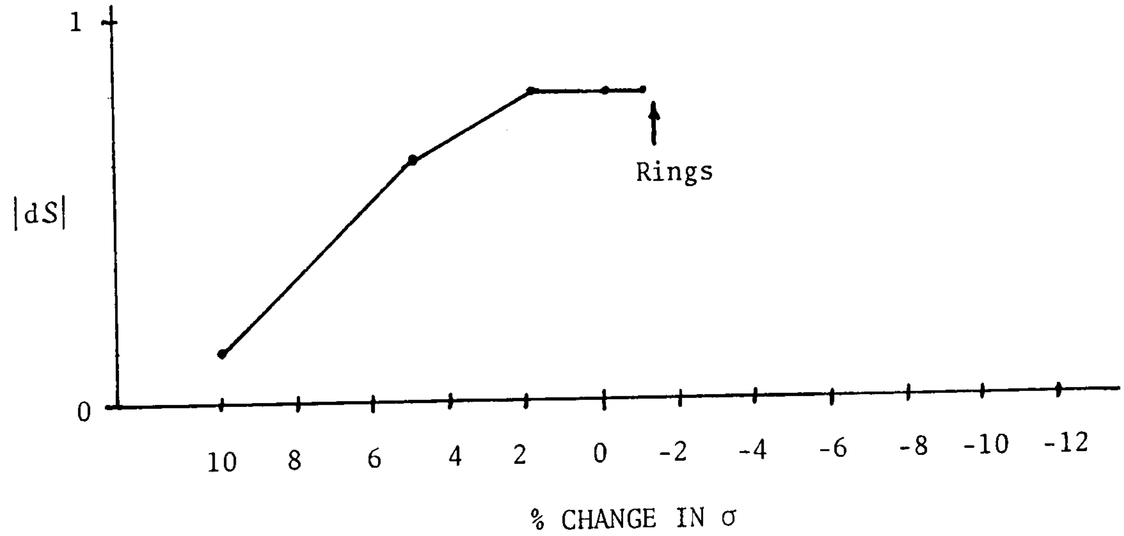

Figure 5-2. Sensitivity of Pole at σ = -0.8566.

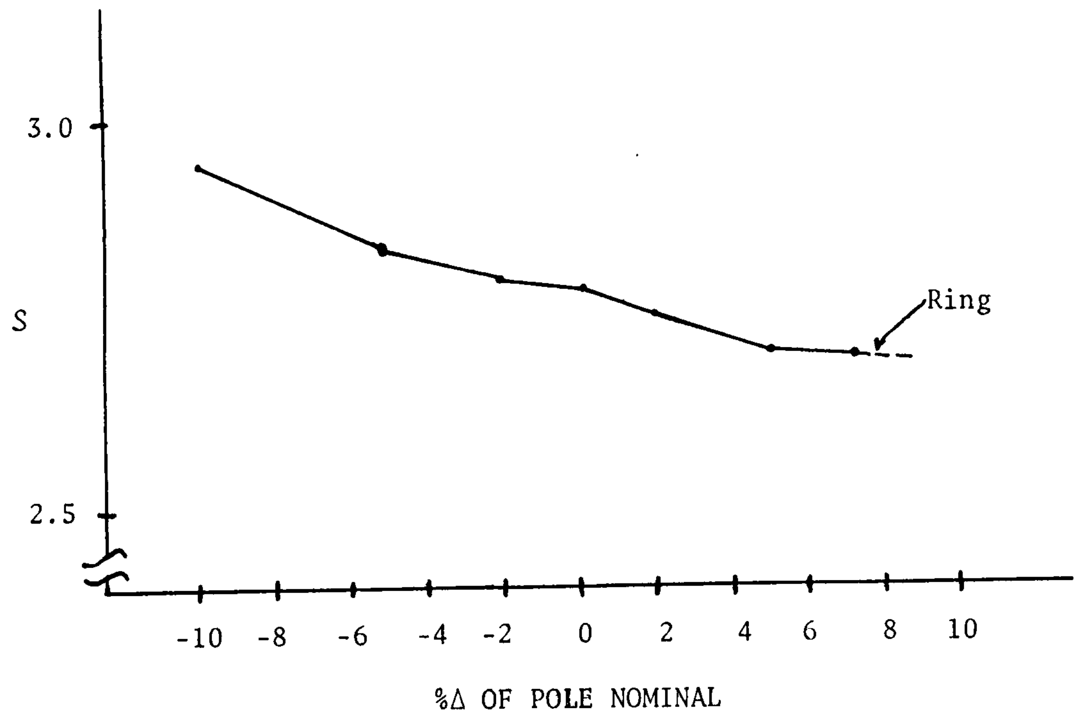

Figure 5-3. Movement of Pole at σ = -1.47.

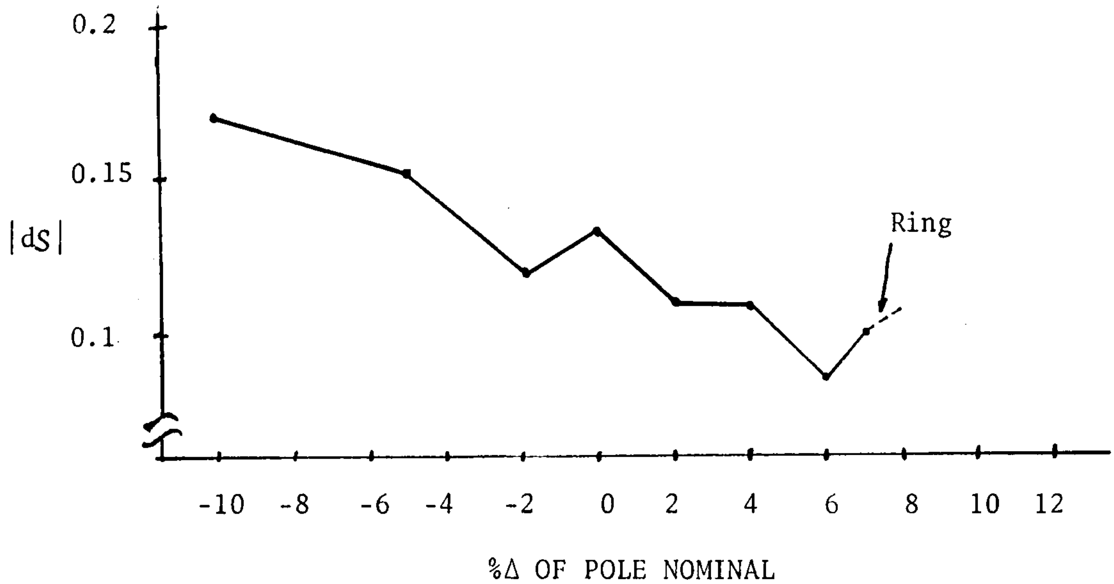

Figure 5-4. Sensitivity of Pole at σ = −1.47.

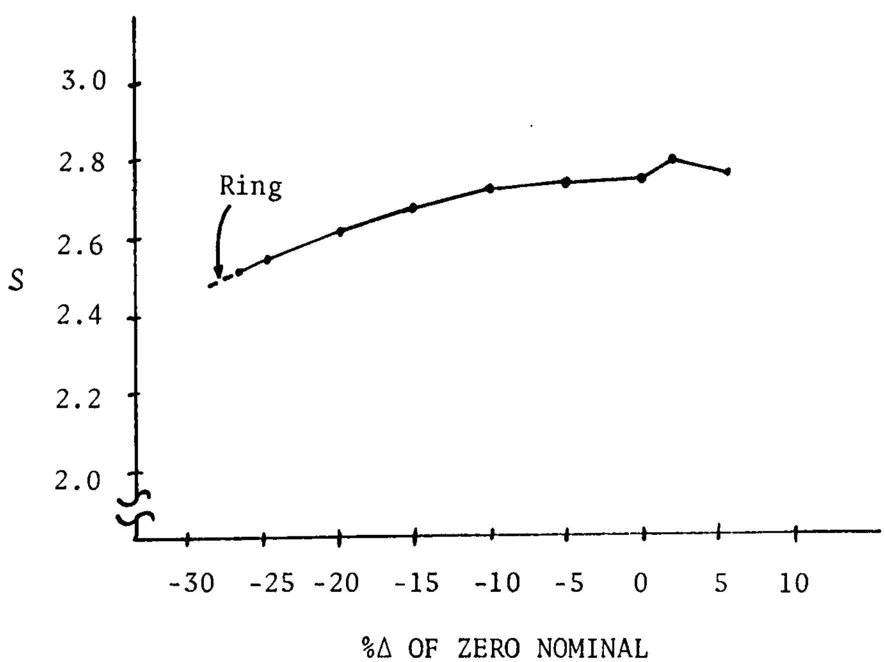

Figure 5-5. Zero Position.

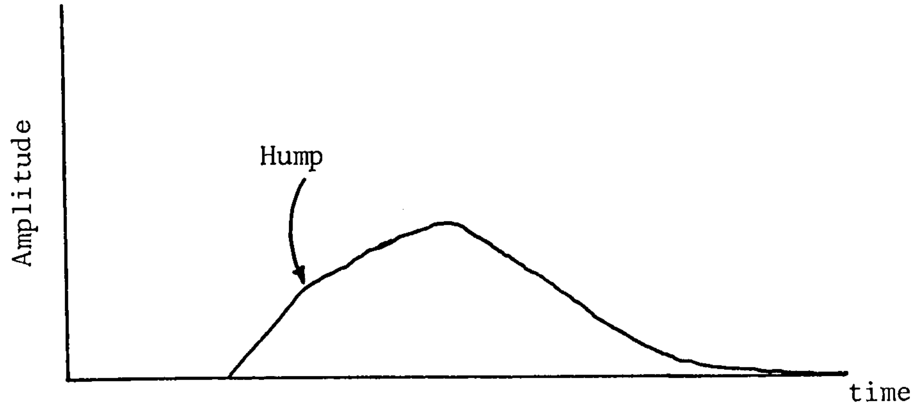

Figure 5-6. Hump Seen in Zero Movement.

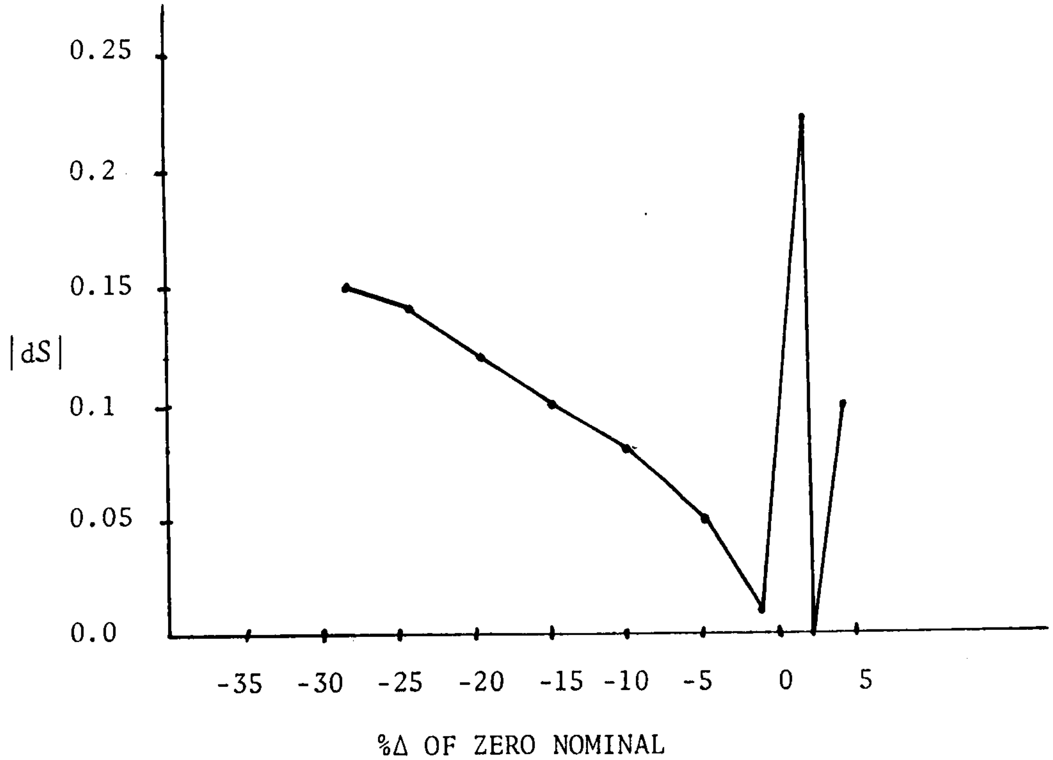

Figure 5-7. Zero Sensitivity.

Figure 5-8 gives the values of the outer pole ($j\omega = \pm j\ 1.162$) plotted against the incremental ω. This pole is not overly effective as it is moved by varying ω. At -2% the value of the shape factor is at a minimum. Further movement will cause ringing. Figure 5-9 shows that the sensitivity is approaching a low value as the shape factor approaches a minimum. This fact would tend to enhance the use of this pole movement for decreasing the shape factor.

Figure 5-10 illustrates the shape factor for movements along the σ axis ($\sigma = -0.9015$) of the outer poles. Up to now almost any movement past the minimum of the shape factor would cause ringing on the waveform. The σ movement of the outer poles shows no such ringing. The minimum shape factor occurs in the neighborhood of -5%. At this value the sensitivity is of course equal to zero and the shape factor is 2.765. The sensitivity is graphed in Figure 5-11.

Figures 5-12 through 5-15 show the inner pole ω and σ movements. Figure 5-12 gives the shape factor for movement of the inner pole ($j\omega = \pm j\ 1.051$). The shape factor is lowest in the neighborhood of +2.5% of ω. The sensitivity at this point is also low. These two facts combined indicate that the adjustment of this pole component should be considered strongly due to the sensitivity of Figure 5-13. Figures 5-14 and 5-15 show the effects of adjusting the σ component of the inner poles ($\sigma = -0.875$). The sensitivity of such an adjustment is extremely high compared to the other poles and zeros and therefore should not be considered.

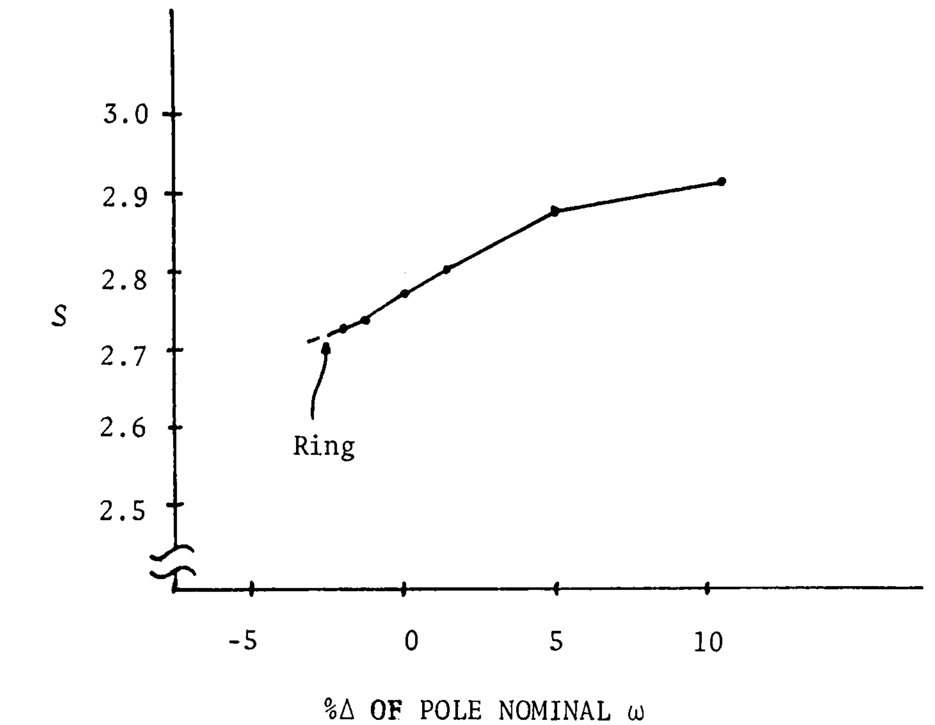

Figure 5-8. Outer Pole ω Movement.

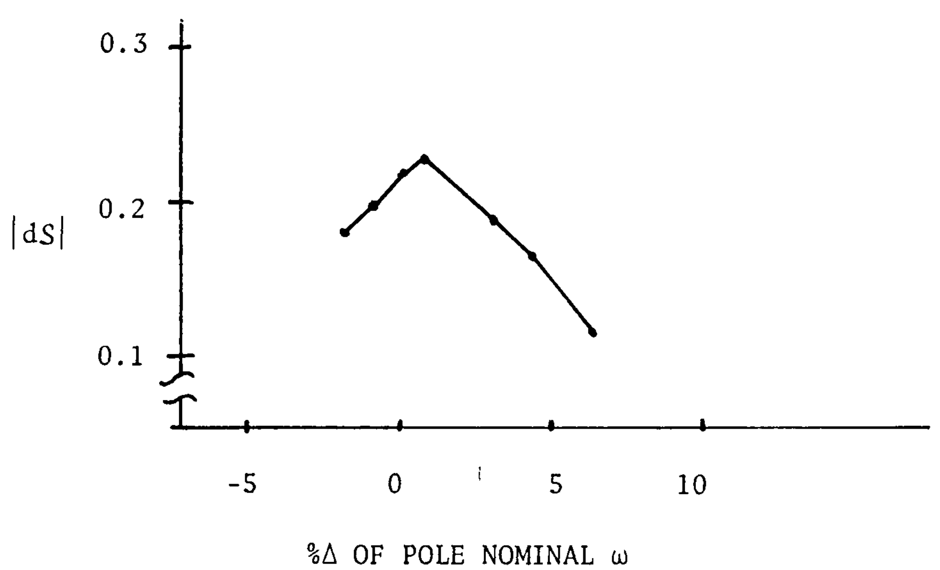

Figure 5-9. Outer Pole ω Sensitivity.

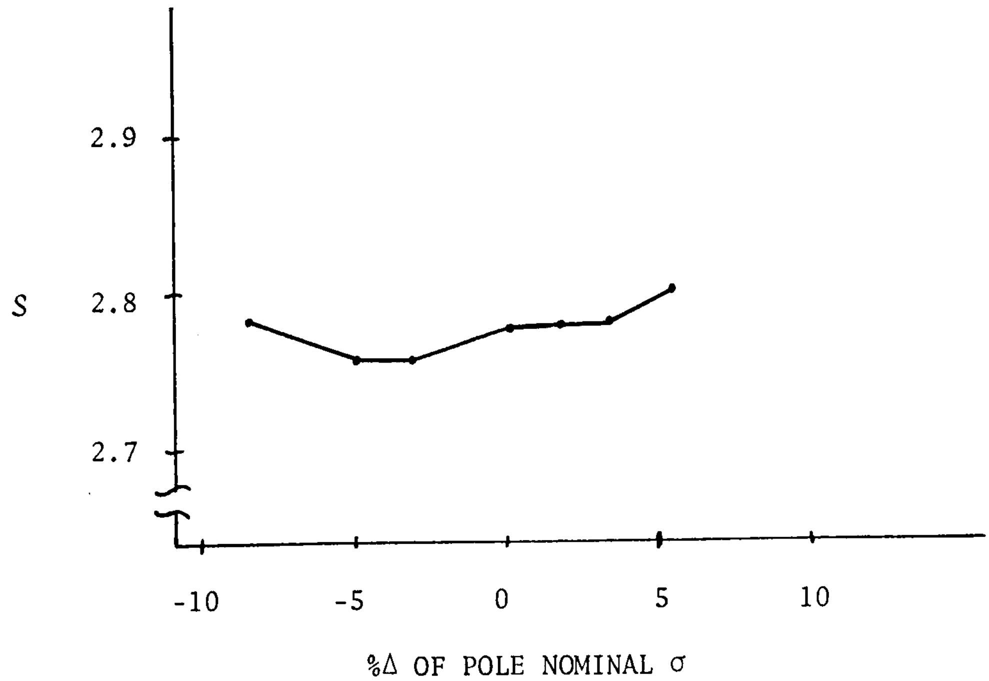

Figure 5-10. Outer Pole σ Movement.

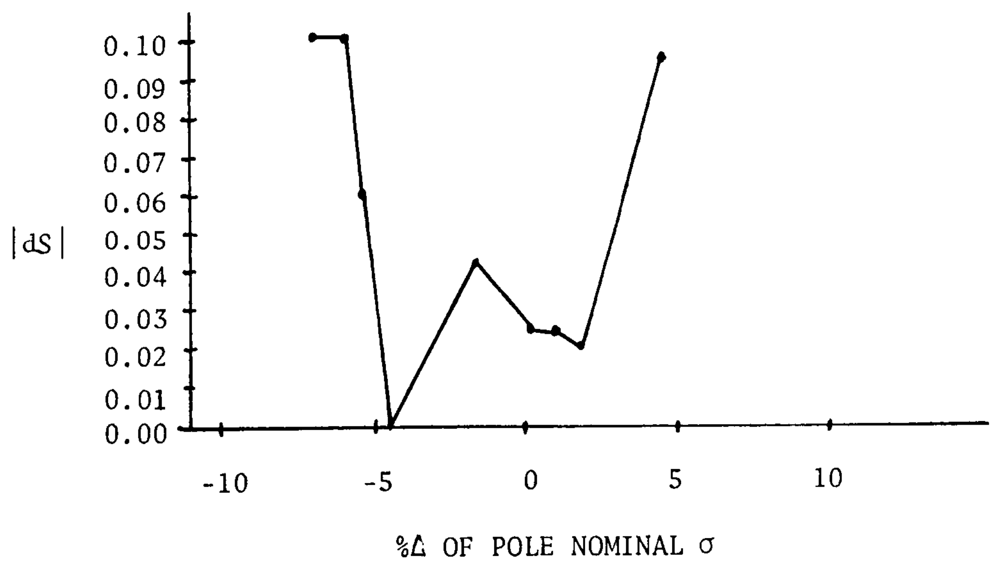

Figure 5-11. Outer Pole σ Sensitivity.

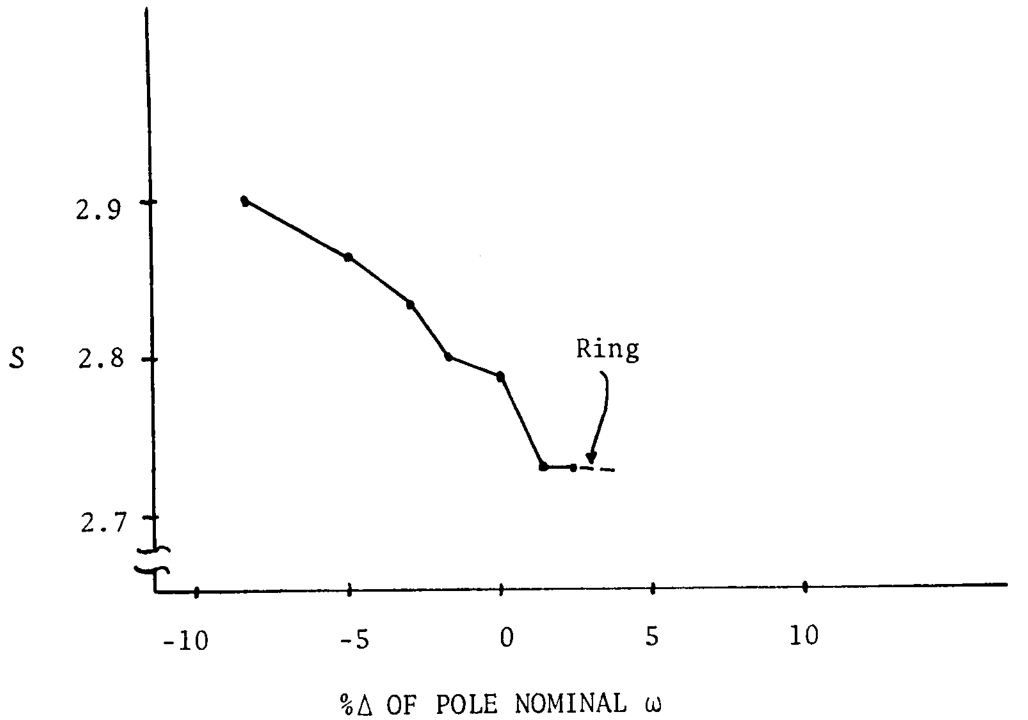

Figure 5-12. Inner Pole ω Movement.

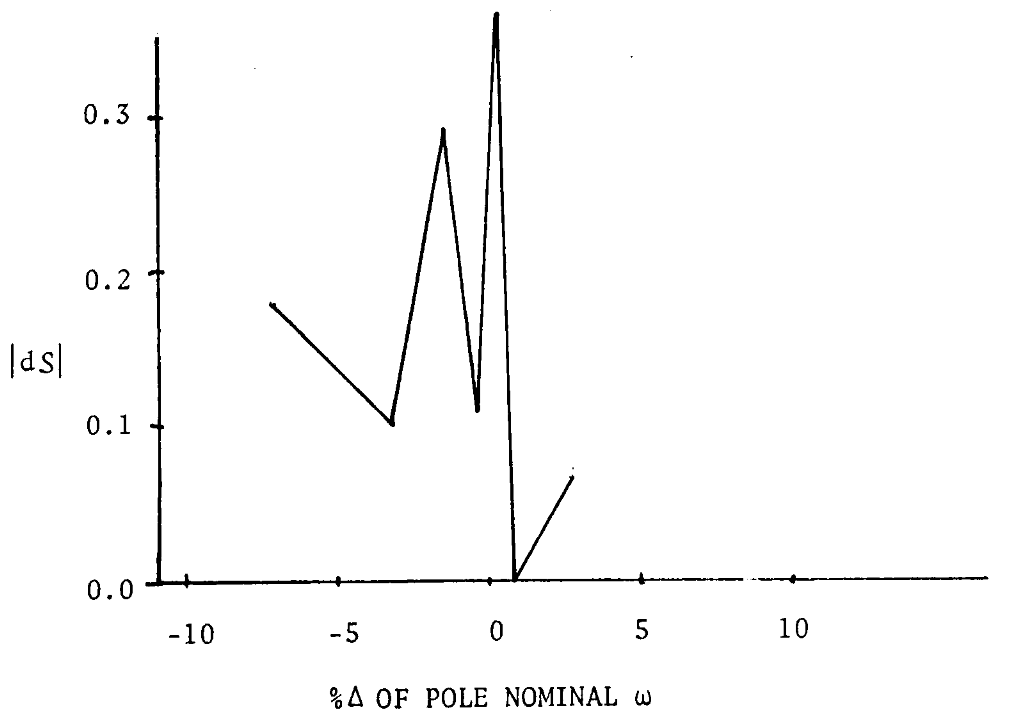

Figure 5-13. Inner Pole ω Sensitivity.

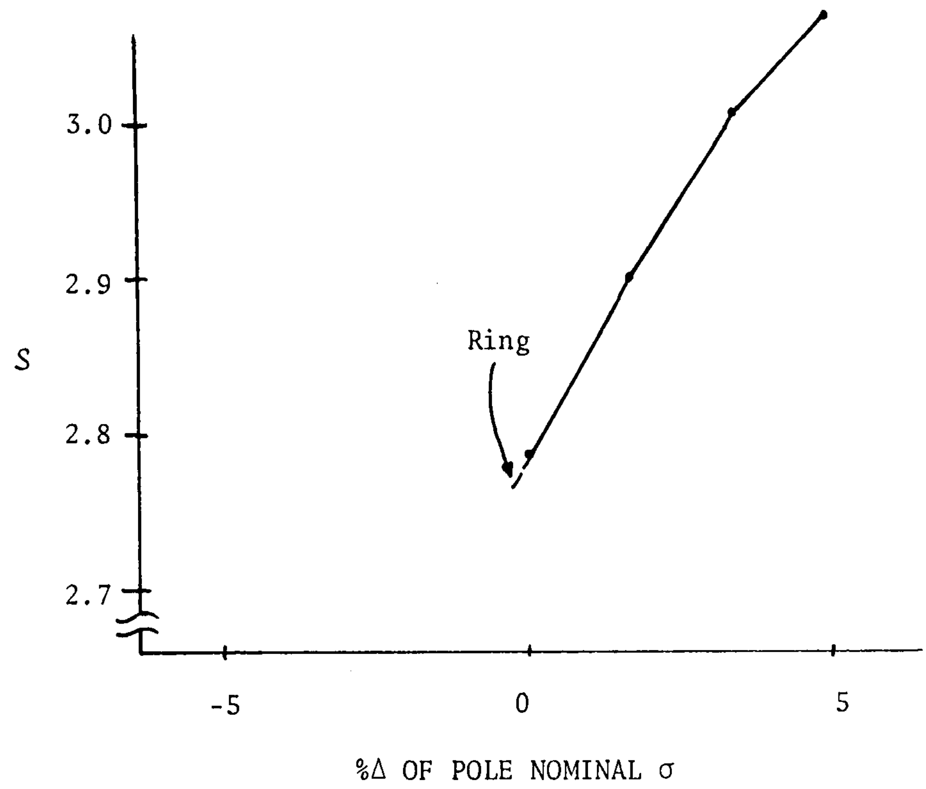

Figure 5-14. Inner Pile σ Movement.

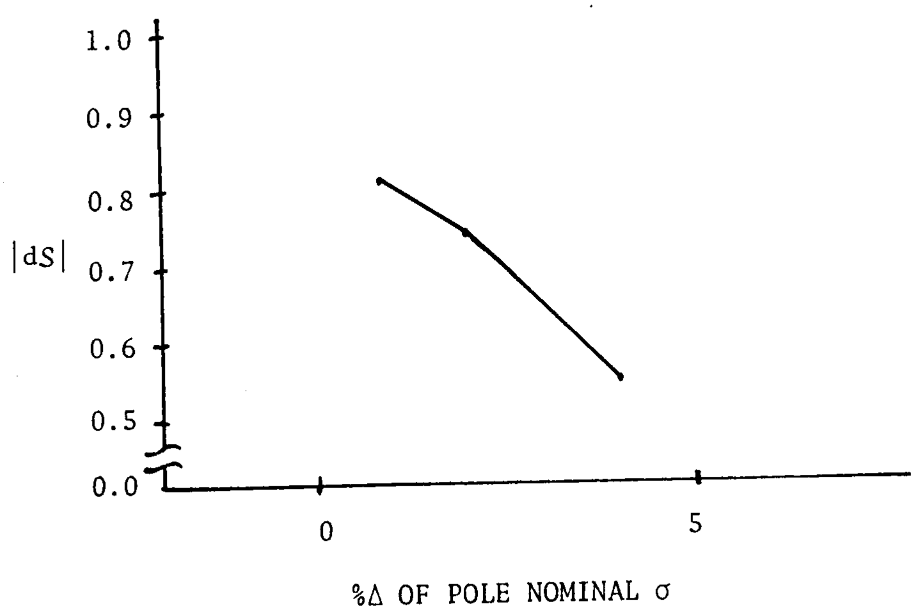

Figure 5-15. Inner Pole σ Sensitivity.

These data indicate that several improvements can be made on the symmetry of the impulse response of the filter. Care must be taken not to allow the poles and zeros to vary over a large range. If the poles or zeros vary, the shape factor will be adversely affected. A serious problem will exist if the poles or zeros drift into the range of values for which the impulse response rings. False triggerings of associated data processing electronics could occur.

The shape factor by itself is not a useful criteria for evaluating a filter. The pulse duration and noise performance must be considered along with the shape factor. As will be seen in the next chapter, the pulse duration will be determined by the optimum cusp factor caluclations. Chapter VII will combine all three indicators to determine the optimum filter of those considered.

In summary, this chapter has presented data from sensitivity calculations of the various poles and zeros of the C. B. 1. The sensitivities of the shape factor S versus pole and zero positions were computed. Some of the sensitivities were found to have regions in which the impulse response of the filter would have excess peaks or ringing. These regions would not be a desirable location for the poles or zeros. The pole-zero positions which have been found to have the best shape factors will be analyzed with respect to noise performance in Chapter VI. The various filters will then be examined for overall time-noise performance.

CHAPTER VI

FILTER NOISE PERFORMANCE

One of the major factors in choosing a filter for pulse spectroscopy is its noise performance. This chapter will be concerned with the theoretical performance of the optimized filters presented in the last chapter. The noise performance of the filters will be compared to that of the optimum cusp. This comparison will generate numbers which are called the cusp factors. The cusp factors of the C. B. 1 filters will then be compared to the cusp factors of the Nowlin filters.

The optimum cusp or infinite cusp as it is also known has an impulse response[14]

$$h(t) = e^{-\alpha|t|} \quad , \; -\infty < t < \infty \qquad (6\text{-}1)$$

where α is referred to as the noise-corner frequency. This noise-corner frequency, or simply noise-corner, is the frequency at which the white noise is equal to the ω^{-2} noise in a charge-sensitive preamplifier. A discussion of the sources of these types of noise will not be attempted here. The reader is referred to Blalock[15] and Millard[16] for a complete discussion of this subject.

The infinite cusp is obviously not practical to synthesize because it is a noncausal response. The signal extends from $-\infty$ to $+\infty$. This cusp serves only as a standard by which to compare other pulses with respect to noise-to-signal ratio. The minimum noise-to-signal ratio for this pulse is

$$NSR_c = K\sqrt{2\alpha} \tag{6-2}$$

where K is a constant which will be defined later. This equation is valid only when the pulse response is optimized for the system in which it is used.

The method of noise calculation used by Nowlin will be used here also because this comparison is to be a direct comparison. The basic system diagram used by Nowlin is shown in Figure 6-1. This model assumes that the output signal from the semiconductor radiation detector is a current impulse. The charge-sensitive preamplifier is modeled as a transfer impedance which has one real pole and no finite zeros. The input noise power spectral density (NPSD) is assumed to have only white and ω^{-2} components due to the input of the amplifier. Nowlin[17] and Millard[18] conclude that the output NPSD of the charge-sensitive preamplifier is

$$NPSD_{CSP} = \frac{K^2(\omega^2+\alpha^2)}{\omega^2 + b^2} \tag{6-3}$$

where α is the noise corner, b is the real pole of the charge-sensitive preamplifier, and K is a noise amplitude constant.

The block labeled "Pole-Zero Cancellation Network" is a conceptual network that cannot exist in reality. The pole that would normally be found with the zero has been lumped with the final block.

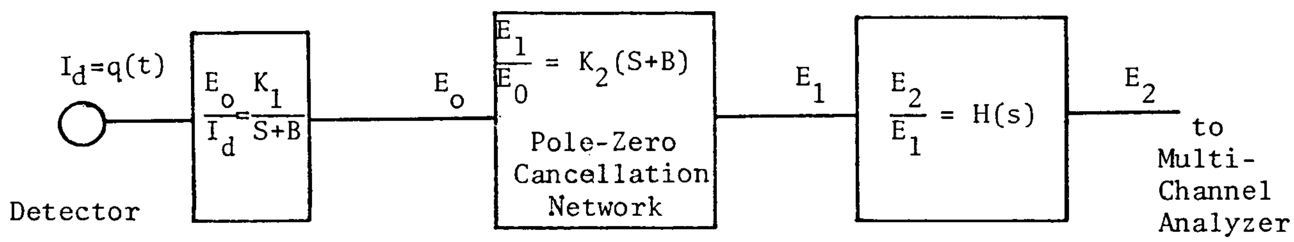

where H(s) is the filter transfer function under consideration

Figure 6-1. System Used by Nowlin.

This is done for flexibility and ease of calculation. The improvement in performance shown by pole-zero cancellation was discussed by Nowlin and Blankenship.[19]

After pole-zero cancellation the NPSD of the input signal to the shaping amplifier will be

$$\mathrm{NPSD} = K^2(\omega^2 + \alpha^2) \qquad (6\text{-}4)$$

due to the cancellation of the real pole in the charge-sensitive preamplifier by the pole-zero cancellation. Letting $H(j\omega)$ equal the transfer function of the amplifier under consideration, the total noise output of the system will be

$$N_0 = \frac{K^2}{2\pi} \int_{-\infty}^{\infty} |H(j\omega)|^2(\alpha^2+\omega^2)\,d\omega \qquad (6\text{-}5)$$

The limits of Equation (6-5) extend to $-\infty$ because the infinite cusp must be evaluated as a two-sided Laplace transform due to the noncausal nature of the cusp.

Equation (6-5) can be expanded into two equations; I_0 and I_2. I_0 is defined as

$$I_0 = \frac{K^2}{2\pi} \int_{-\infty}^{\infty} \alpha^2|H(j\omega)|^2 d\omega \qquad (6\text{-}6)$$

I_2 is defined as

$$I_2 = \frac{K^2}{2\pi} \int_{-\infty}^{\infty} |\omega H(j\omega)|^2 d\omega \qquad (6\text{-}7)$$

Now let

$$J_0 = \frac{I_0}{K^2\alpha^2} \tag{6-8}$$

and

$$J_2 = \frac{I_2}{K^2} \tag{6-9}$$

for calculation purposes. I_0 is the total output noise power resulting from white noise at the input of the filter and I_2 is the output power resulting from ω^2 noise at the input to the filter. Rewriting Equation (6-5)

$$N_0 = K^2(\alpha^2 J_0 + J_2) \tag{6-10}$$

If all of the poles p_i and zeros z_i are replaced by ηp_i and ηz_i respectively, where η is a constant, the total output noise power becomes, for constant peak amplitude of the impulse response

$$N_0(\eta) = K^2\left[\frac{\alpha^2 J_0}{\eta} + \eta J_2\right] \quad . \tag{6-11}$$

Taking the derivative of $N_0(\eta)$ with respect to η, Equation (6-11) becomes

$$\frac{dN_0(\eta)}{d\eta} = \frac{-K^2\alpha^2 J_0}{\eta^2} + K^2 J_2 \tag{6-12}$$

Setting Equation (6-12) equal to zero, Equation (6-13) becomes the value of η for which $N_0(\eta)$ is minimized.

$$\eta_0 = \alpha\left(\frac{J_0}{J_2}\right)^{\frac{1}{2}} \qquad (6\text{-}13)$$

To optimize the original $H(j\omega)$ with respect to the noise corner α, Equation (6-13) is evaluated for a particular $H(j\omega)$ and α. The poles and zeros are then replaced by η times the poles and zeros.

The cusp factor will now be quantitatively defined. Equation (6-2) is the minimized noise-to-signal ratio for the cusp. In the full form, NSR for any system is

$$\mathrm{NSR} = \frac{(\text{Output Noise Power})^{\frac{1}{2}}}{h(t)_{max}}\ , \qquad (6\text{-}14)$$

where $h(t)_{max}$ is the peak of the impulse response. For the cusp, $h(t)_{max}$ equals one for all values of α at $t = 0$. The cusp factor is then defined as

$$\mathrm{CF} = \frac{\mathrm{NSR}_{\text{System Under Consideration}}}{\mathrm{NSR}_c} \qquad (6\text{-}15)$$

Optimizing J_0 and J_2 according to Equation (6-13), the cusp factor can be written as

$$CF = \frac{\sqrt{K^2\left[\dfrac{\alpha^2 J_0}{\alpha\left(\dfrac{J_0}{J_2}\right)^{\frac{1}{2}}} + \left(\dfrac{J_0}{J_2}\right)^{\frac{1}{2}} J_2\right]} \Bigg/ h(t)_{max}}{K\sqrt{2\alpha}} \tag{6-16}$$

Simplifying Equation (6-16) gives

$$CF = \frac{(I_0 I_2)^{\frac{1}{4}}}{h(t)_{max}} \tag{6-17}$$

The ratio of the noise line width of a filter to the noise line width of the infinite cusp is given by

$$NLWR = (CF)\left[\frac{1}{2}\left(\frac{\eta_0}{\eta} + \frac{\eta}{\eta_0}\right)\right]^{\frac{1}{2}} \tag{6-18}$$

All data presented in this chapter was calculated for a noise corner α equal to 1 second. This value of α allows a simplification of calculation. Any scaling could be used however.

All integrals were evaluated by the method of residues. The program used is presented in Appendix B. The approximate peak values of the optimized impulse-responses were calculated by the program presented in Appendix C. Table 6-1 presents the data calculated. The C. B. 1 filter and its derivatives from Chapter V all had worse noise performance than the Nowlin N = 5 filter. The C. B. 1 and its derivative optimized

TABLE 6-1

NOISE CALCULATION RESULTS

Type	Factor Adjusted	η	C.F.
Nowlin N = 5	None	2.0388	1.131
Nowlin N = 7	None	2.206	1.135
C. B. 1	None	2.433	1.134
C. B. 1	Zeros by -27%	2.4074	1.257
C. B. 1	Pole at -0.8566 by +1%	2.428	1.138
C. B. 1	Pole at -1.47 by +7%	2.4146	1.139
C. B. 1	Outer pole ω by -2%	2.4428	1.137
C. B. 1	Outer pole σ by -5%	2.4199	1.138
C. B. 1	Inner pole ω by +1.5%	2.425	1.138
C. B. 1	Inner pole σ by 0%	2.43311	1.134

for the inner pole σ time response which are in fact identical had better noise performance than Nowlin's N = 7 filter. Most of the filter derivatives presented had small pole movements. The cusp factors are therefore grouped relatively close together. The single exception to this is the set of complex zeros. They were changed approximately -27%. This large change gave a correspondingly large change in the cusp factor. The reason for the change is obvious in that even though the noise integrals were reduced by the movement, the peak amplitude was reduced even more.

This chapter has presented the theory necessary to determine noise performance of nuclear pulse filters. The equations used assume a white and ω^{-2} noise spectrum generated by the first stage of an FET input charge sensitive preamplifier. The filter noise performance equations compare a filter to the ideal cusp, a practically unrealizable but theoretically useful time response. The equations were developed to facilitate the optimization of the noise performance of a filter with respect to the noise corner, i.e., the frequency at which the white noise component of a charge sensitive preamplifier equals the ω^{-2} noise component. The findings indicate that the original C. B. 1 filter has the best noise performance. The others are only slightly worse. The analysis of Chapter VII will employ the original C. B. 1 as the filter to be compared in overall performance to the Nowlin N = 5.

CHAPTER VII

TOTAL FILTER PERFORMANCE

The goal of this chapter is to combine the results of Chapters V and VI with information presented in this chapter to arrive at some desirable filter configuration. This chapter will present a qualitative explanation of resolution loss due to tail pile up. A number will be generated to compare the resolution of the Nowlin N = 5 filter to one of the C. B. 1 filters.

As counting rates become high, the resolution of the system tends to decrease. The decrease is due mainly to the peak of the pulse being shifted upward in value by the tail of a previous pulse. If the output voltage of the filter is assumed to be V(t), then Campbell's theorems give the mean voltage and the mean-square voltage as[20]

$$\overline{V} = n \int_{-\infty}^{\infty} V(t)dt \tag{7-1}$$

and

$$\overline{V^2} = n \int_{-\infty}^{\infty} V^2(t)dt \tag{7-2}$$

where n is the pulse repetition rate. The pulses will exhibit a mean shift plus some RMS variation. The resolution cannot, therefore, be simply related to the RMS component. A simplified explanation is in order to give some approximation of the loss in resolution due to the pile-up.

Two cases of pile up can be considered here. The difference is rather arbitrary but will serve a useful purpose for this discussion. If the pulse is broken into two distinct parts by voltage level, the matter of pile-up can be greatly simplified. The two parts will arbitrarily be called the peak and the tail. The distinction is illustrated in Figure 7-1. For $0 \leq T < T_a$, the pulse will be considered to be in the peak region. For $T \geq T_a$ the pulse will be considered to be in the tail region.

For two pulses very close together in time, i.e., the peak portion of the second pulse falling within the duration of the peak portion of the first pulse, there will be a gross shift in the peak value of the second pulse and probably also of the first pulse. This kind of shift is easy to prevent with the use of a pile-up rejector. Two peaks falling within a time period $0 \leq T < T_a$ will be rejected. Due to the electronics of a pile-up rejector, two pulses occurring at the same time would probably not be rejected. This kind of gross overload however, would cause the peak to fall outside the range of measurement. The region of interest, therefore, will be for times greater than T_a.

Ignoring the peak portion of the pulse, the remainder of the pulse would resemble an exponential as in Figure 7-2. The point of interest for tail pile-up is point X in Figure 7-2 where X is any instant of time excluding the dotted or peak portion of the waveform.

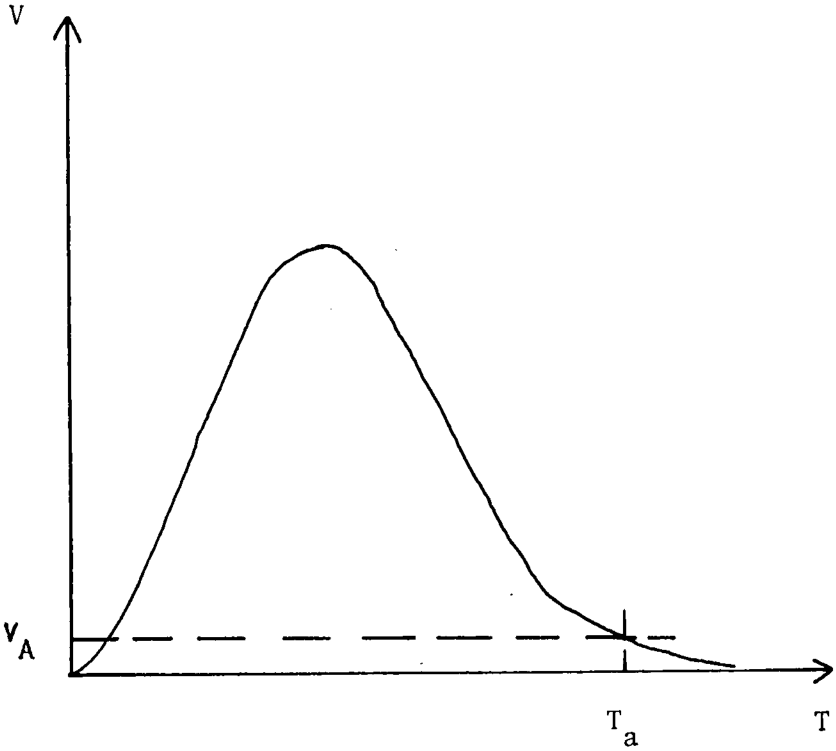

Figure 7-1. Two Part Pulse.

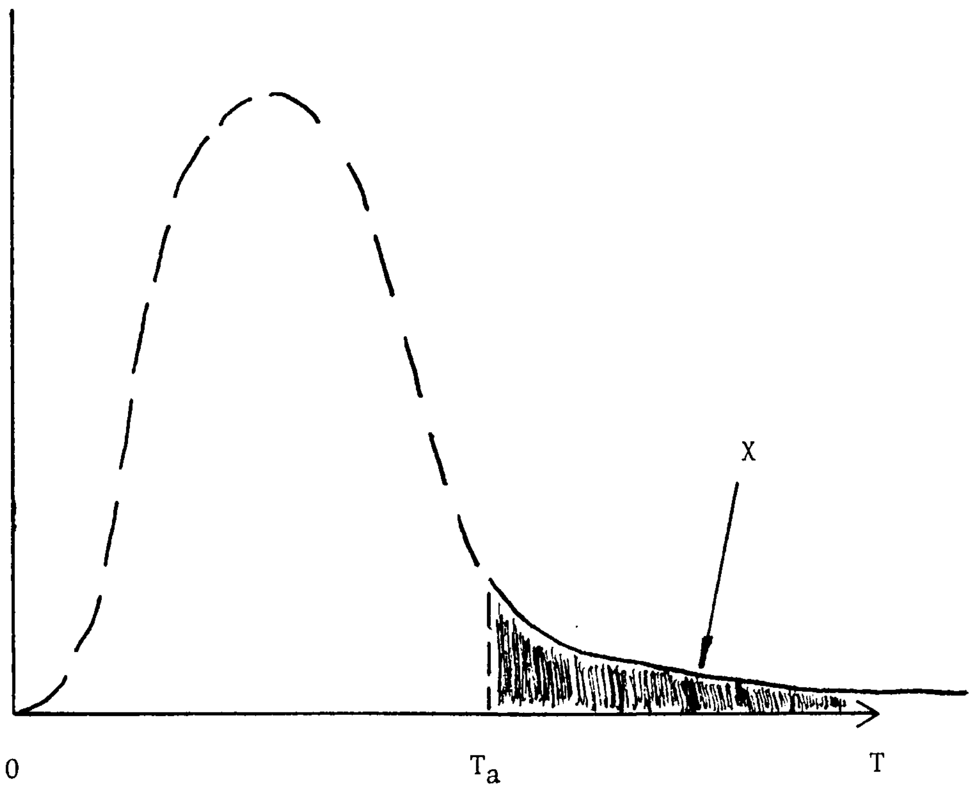

Figure 7-2. Pulse After T_a.

The effect of tail pile-up is for a peak of a later pulse to occur at the point X thus being shifted upward in voltage by the value of this previous waveform at X. The resulting time-response is illustrated in Figure 7-3(a),(b). V is the peak height of both pulses. V is the voltage value of the tail of the first peak at the time of occurrence of the second peak.

The original C. B. 1 has been chosen for examination due to the superior noise performance compared to the other C. B. 1 versions. To approximate a comparison of the loss in resolution, the waveforms being considered must necessarily be simplified. The portions over which the Campbell integrals will be evaluated will be $\tau_{0.1\%}$ and $\tau_{0.0001\%}$ for the C. B. 1 and $\tau_{0.1\%}$ of the C. B. 1 and $\tau_{0.0001\%}$ of the N = 5 for the N = 5. The initial limit is arbitrary but must be equal for both pulses if an accurate comparison is to be performed. The final limit must be chosen so that the integrals can be seen to be converging. These limits satisfy this requirement. A practical realization of the situation being evaluated is to set a pile-up rejector so that any peaks of a second pulse occurring during the time interval $0 \leq T < T_a$ of the first pulse would be rejected. The situation is illustrated in Figure 7-4. The integral programs can be found in Appendix D.

The value of the mean voltage for a 3.62 second peaking time is

$$\overline{V} = n \int_{9.9\text{ sec}}^{17.9\text{ sec}} V(t)dt = n(1.902 \times 10^{-3} V\text{-}S) \qquad (7\text{-}3)$$

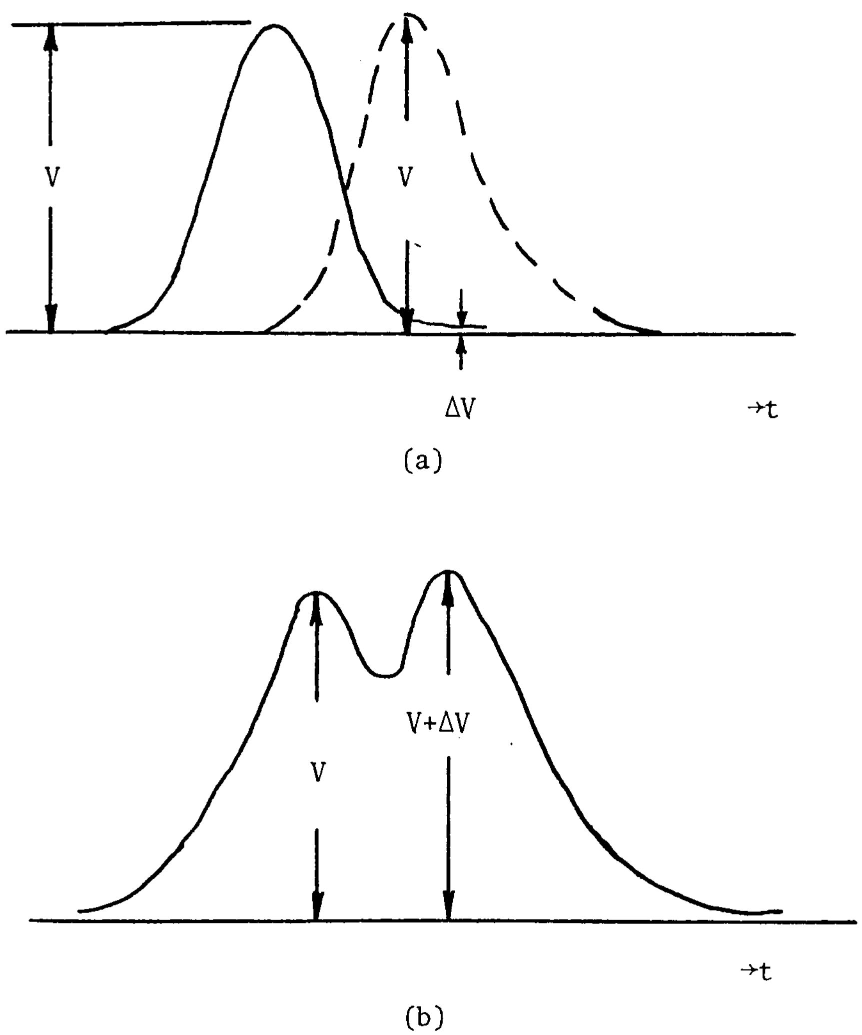

Figure 7-3. Effect of Pile Up.

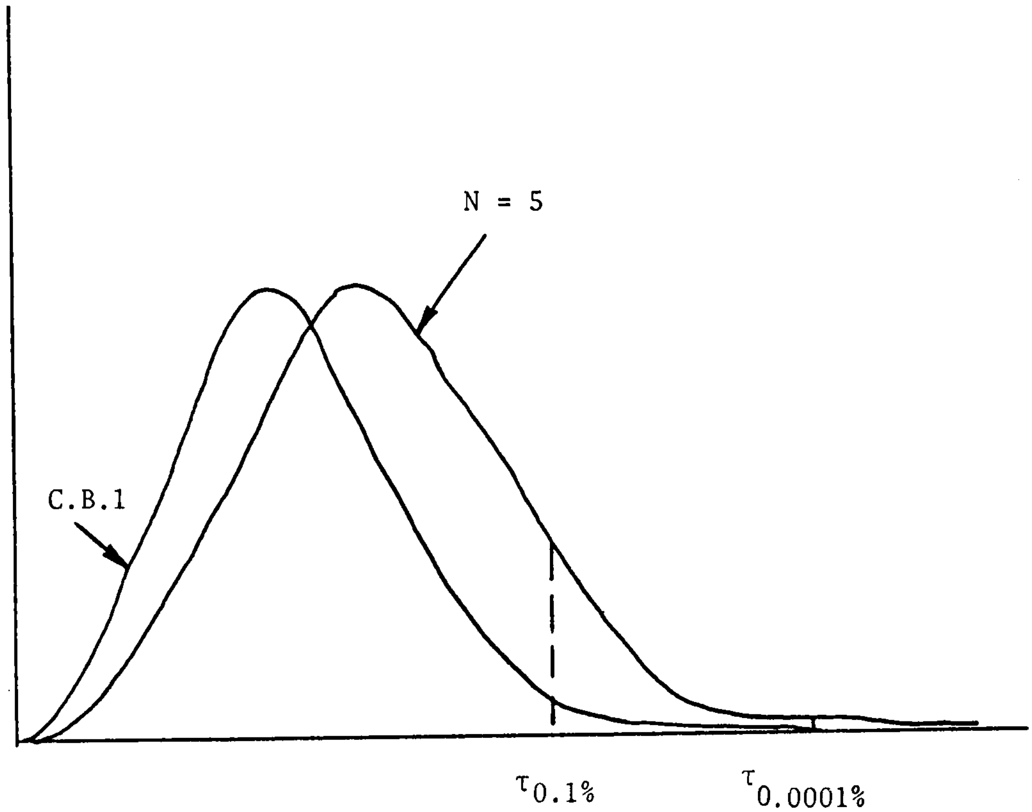

Figure 7-4. C. B. 1, N = 5 Comparison.

and for the N = 5 for a peaking time of 3.77 seconds

$$\overline{V} = n \int_{9.9\ \text{sec}}^{21.05\ \text{sec}} V(t)dt = n(6.639 \times 10^{-3} V\text{-}S) \tag{7-4}$$

where n is the counting rate. If $n = 4.56 \times 10^{-2}$ cps, which is equivalent to a 50Kcps count rate for 2 μsec. shaping, $\overline{V}$ will be for the C. B. 1

$$\overline{V} = (4.56 \times 10^{-2})(1.902 \times 10^{-3}) = 8.67 \times 10^{-5} V \tag{7-5}$$

Since there is a 1V peak, the percent peak shift becomes

$$\frac{8.67 \times 10^{-5}}{1} \times 100\% = 0.0087\% \tag{7-6}$$

and similarly for the N = 5

$$\%\ \text{Shift} = 0.030\% \tag{7-7}$$

which is 3.5 times worse than the C. B. 1. The mean-square variation about these means are calculated for the C. B. 1 as

$$\overline{V^2} = n \int_{9.9\ \text{sec}}^{17.9\ \text{sec}} V^2(t)dt = n(9.51 \times 10^{-7} V^2\text{-}S) \tag{7-8}$$

and for the N = 5

$$\overline{V^2} = n \int_{9.9\ \text{sec}}^{21.05\ \text{sec}} V^2(t)dt = n(1.17 \times 10^{-5} V^2\text{-}S) \tag{7-9}$$

For the same count rate as before the V_{RMS} for the C. B. 1 is

$$V_{RMS} = 2.1 \times 10^{-4} V \qquad (7\text{-}10)$$

and for the N = 5

$$V_{RMS} = 7.3 \times 10^{-4} V \qquad (7\text{-}11)$$

The N = 5 is therefore 3.5 times worse on this parameter also.

Thus far the cases of minimized noise have been studied. According to Equation (6-18) the peaking time of a filter can be either lengthened or shortened with a corresponding decrease in noise performance. If the cusp factor of the N = 5 is allowed to equal 1.134, which is the cusp factor of the C. B. 1, the peaking time can be shortened by 9.8%. The average voltage now becomes

$$\overline{V} = n \int_{9.9\ \mathrm{sec}}^{19\ \mathrm{sec}} V(t)dt = n(3.47 \times 10^{-3} V\text{-}S) \qquad (7\text{-}12)$$

Equation (7-12) is 1.82 times worse than the C. B. 1 which is an improvement over the first N = 5 case but still worse than the C. B. 1. The mean-square variation is likewise

$$\overline{V^2} = n \int_{9.9\ \mathrm{sec}}^{19\ \mathrm{sec}} V^2(t)dt = n(3.397 \times 10^{-6} V^2\text{-}S) \qquad (7\text{-}13)$$

Comparing V_{RMS} of the N = 5 to V_{RMS} of the C. B. 1 gives

$$\frac{V_{RMS}^{N=5}}{V_{RMS}^{C.B.1}} = 1.89 \tag{7-14}$$

This result also indicates that the high count rate performance of the C. B. 1 is better than that of the N = 5.

As stated earlier, this method is an approximation and should be taken as a qualitative comparison of the effects of tail pile-up. The absolute values as calculated should be relatively close to the real value. The ratios should be even closer since the ratios are comparing relative areas under the tails. The relative areas are indicators of performance concerning baseline shifts due to pile-up.

In conclusion, the longer, steeper tail of the N = 5 will have an appreciable effect on the tail pile-up and therefore the resolution of the system. The C. B. 1 with its shorter peaking time and quicker return to baseline should have a better resolution as far as peak shift and peak broadening. The improvement over the N = 5 should be on the order of 3.5 times. This result could be generalized to any filter type. The methods used could also be implemented to give a comparison between the filters considered and other filters. Even shortening the N = 5 pulse length to equal the noise performance of the C. B. 1 does not allow the N = 5 to equal the high count rate performance of the C. B. 1.

For overall performance, the C. B. 1 would seem to be the choice for most nuclear applications since most modern day systems require higher and higher count rates. The noise line width at FWHM (Full

Width at Half Maximum) would be approximately 3 channels out of 1000 wider for the C. B. 1 than for the N = 5 filter. At very high count rates there would be a measurable difference between the peak shift and resolution of the N = 5 and C. B. 1. The C. B. 1 version of the C. B. 1 modifications was chosen due to its cusp factor. Since the shapes of the C. B. 1 versions are similar, there would be very little difference between the time response performances. One very interesting fact should be mentioned. In reducing the peaking time of the N = 5 filter by 9.8%, the cusp factor was only changed by 0.27%. Based on the properties of Equation (6-18), a statement could be made that noise-to-signal ratio is relatively insensitive to a change η. This fact could be useful for optimizing a particular pole-zero constellation to a particular system.

In summary, a qualitative method for estimating the relative count rate performance of the C. B. 1 and the Nowlin N = 5 filters has been described. The method is an approximation of filter performance by waveform modification. The method assumes that a pile-up rejector is included in the system. The rejector in essence limits the amount of a pulse waveform that following waveforms see. This allows a calculation of relative peak shift and peak broadening. The results obtained from the calculations indicate that the N = 5 will have approximately 3.5 times the line broadening and peak shift of the C. B. 1. Combined with the fact that the C. B. 1 has only 0.27% worse noise performance than the N = 5, the choice to use the C. B. 1 was made. For equal noise performance the N = 5 was found to have $\overline{V}$ and

V_{RMS} of 1.82 times worse and 1.89 times worse respectively than the C. B. 1. On this basis the C. B. 1 was also chosen. The C. B. 1 should be a better all around filter for most purposes, especially at the higher count rates of modern spectroscopy systems.

CHAPTER VIII

CONCLUSIONS

I. GENERAL SUMMARY

In this thesis, a theoretical comparison between a filter developed by C. H. Nowlin and a new filter, developed by the author, called the C. B. 1, was presented. The background of nuclear pulse shaping methods was outlined followed by the desired time-domain characteristics of a semi-Gaussian filter. A limited sensitivity study was then undertaken to determine if the time-response characteristics of the C. B. 1 could be improved. Several cases were found which gave only a slight (< 3%) improvement in shape factor S. The shape factor in itself is not useful but must be examined with other criteria present. The noise performance was then computed for the optimized filter. The figure of merit used for noise performance was the cusp factor which relates the noise performance of a filter to that of the ideal cusp. The cusp factor of the C. B. 1 was found to be 1.134 while that of the Nowlin N = 5 filter was 1.131, a difference of only 0.27%. Since the noise line width of a filter is proportional to the cusp factor, this small difference would show up as approximately 3 lines out of 1000 wider than for the N = 5.

The original C. B. 1 was then taken to be the best filter due to its lowest noise configuration. The configuration was analyzed then for the best pile-up performance. The analysis was a qualitative method best suited for a comparative study. The basis of the method was an arbitrary separation of the pulse waveform into a peak portion and a tail portion. The case of peak pile-up was ignored based on the use of a pile-up rejector. The comparative tail pile up was then studied. The parameters considered were peak shift and peak spreading due to the mean tail voltage and the RMS variation respectively. The N = 5 was found to be 3.5 times worse in both respects. This difference should be an indicator of high count rate performance. The noise performance of the N = 5 was set equal to the C. B. 1 in order to shorten the peaking time of the N = 5. The high count rate peak shift was found to be 1.81 times worse than the C. B. 1 and the peak spreading was found to be 1.89 times worse than the C. B. 1.

Based on the slight difference in noise performance and the larger difference in high count rate performance, the conclusion of this thesis is that the C. B. 1 should be somewhat superior to the N = 5 filter for optimized noise performance.

II. AREAS FOR FURTHER STUDY

Based on the findings of this thesis, further study of the C. B. 1 filter should include experimental noise and count rate verification. Higher order constellations of poles would be a useful area of study in that significant improvements over Nowlin N = 7 filter could possibly be found.

Further study in the area of Transversal filters would appear to be a fruitful venture. With the advent of faster charge coupled devices, transversal filtering would appear to be a significant improvement over RLC realizations of impulse response. Surface-acoustic wave devices[21] are also a possibility to replace the charge-coupled devices at higher frequencies.

LIST OF REFERENCES

LIST OF REFERENCES

1. Nowlin, C. H., "Pulse Shaping for Nuclear Pulse Amplifiers," IEEE Transactions on Nuclear Science NS-17 (1), pp. 226-241 (1970).

2. Nowlin, p. 227.

3. Nicholson, P. W., Nuclear Electronics, pp. 97-108, John Wiley (1974).

4. Miller, G. L., and D. A. H. Robinson, "Transversal Filters for Pulse Spectroscopy," IEEE Transactions on Nuclear Science NS-22 (5), pp. 2022-2032 (1975).

5. Nicholson, pp. 108-109.

6. Nowlin, p. 238.

7. Nicholson, p. 146.

8. Nicholson, p. 109.

9. Nowlin, p. 231.

10. Henderson, K. W. and W. H. Kautz," Transient Responses of Conventional Filters," IRE Transactions on Circuit Theory, Dec. 1958, pp. 333-347.

11. Green, Walter, unpublished notes.

12. Karlovac, Neven, private communication.

13. Graeme, J. G., G. E. Tobey and L. P. Huelsman, Operational Amplifiers Design and Applications, McGraw-Hill (1971).

14. Nowlin, p. 227.

15. Blalock, T. Vaughn, "Optimization of Semiconductor Preamplifiers for Use with Semiconductor Radiation Detectors," Ph. D. Dissertation, The University of Tennessee, Knoxville, Tennessee, 1965.

16. Millard, J. K., "An Investigation of Broadband Current Preamplification for Obtaining Simultaneous High-Resolution Energy and Time Information from Nuclear Radiation Detectors," Ph. D. Dissertation, The University of Tennessee, Knoxville, Tennessee, 1971.

17. Nowlin, p. 227.

18. Millard, p. 17.

19. Nowlin, C. H., and J. L. Blankenship, "Elimination of Undesirable Undershoot in the Operation and Testing of Nuclear Pulse Amplifiers," Rev. Sci. Instr. 36, 1830-39 (Dec. 1965).

20. Nicholson, pp. 150-154.

21. Millard, J. K., private communication.

22. James, H. M., N. B. Nichols and R. S. Phillips, Theory of Servo-Mechanisms, Boston Technical Lithographers (1963).

APPENDICES

APPENDIX A

The computer programs for the three filters are straightforward C.S.M.P. programs. For the C. B. 1 the program was:

```
//CB        JOB (******,******,G-X),BRITTON
// EXEC CSMP
//SYSIN DD *
METHOD RKSFX
      INPUT=EXP(TIME/(-.6765))*STEP(0.1)
      X2=INPUT*6.6925
      X3=REALPL(0.,1.1674,X2)
      X4=CMPXPL(0.,0.,.61311,1.4709.X3)
      X5=X4-1.75*X7-1.187*X8
      X6=X5
      X9=X6+2.4797*X8
TIMER FINTIM=20. ,DELT-.005  ,PRDEL-.1 ,OUTDEL=.1
PRTPLT X9
END
STOP
ENDJOB
```

For Nowlin's N = 5 filter:

```
//CB        JOB(******,******,G-X),BRITTON
// EXEC CSMP
//SYSIN DD *
METHOD RKSFX
      INPUT=EXP(TIME/(-.7143))*STEP(0.)
      X2=INPUT*5.6696
      X3=REALPL(0.,1.1429,X2)
      X4=CMPXPL(0.,0.,.74329,1.177,X3)
      X5=X4-1.75*X7-3.2462*X8
      X6=X5
      X7=INTGRL(0.,X6)
      X8=INTGRL(0.,X7)
      X9=X6+4.0501*X8
TIMER FINTIM=20. ,DELT=.005  ,PRDEL-.1 ,OUTDEL=.1
PRTPLT X9
END
STOP
ENDJOB
```

For Nowlin's N = 7 filter:

```
//NOWL     JOB(******,******,G-X),BRITTON
// EXEC CSMP
//SYSIN DD *
METHOD RESFX
      INPUT=EXP(TIME/(-1))*STEP(0.)
      X2=INPUT*17.126
      X3=REALPL(0.166667.X2)
      X4=CMPXPL(0.,0.,.48565,2.0591,X3)
      X5=X4-2.*X7-1.36*X8
      X6=X5
      X7=INTGRL(0.,X6)
      X8=INTGRL(0.,X7)
      X9=X6+3.24*X8
      X10=CMPXPL(0.,0.,.64018,1.562,X9)
TIMER FINTIM-20. ,DELT=.005  ,PRDEL=.1 ,OUTDEL=.1
PRTPLT X9
END
STOP
ENDJOB
```

The programs are mostly a straightforward application of C.S.M.P. except for the final parts of the bodies. These are a state variable approach which synthesizes complex poles and complex zeros. The transfer functions are easily calculated from flow graph theory.

APPENDIX B

The following program will calculate the integral for the general equations

$$I_0 = \frac{1}{2\pi} \int_{-\infty}^{\infty} |H(j\omega)|^2 d\omega \qquad \text{(B-1)}$$

and

$$I_2 = \frac{1}{2\pi} \int_{-\infty}^{\infty} |\omega H(j\omega)|^2 d\omega \quad . \qquad \text{(B-2)}$$

The form of the equation must be

$$H(s) = \frac{B_0 S^{10} + B_1 S^8 + B_2 S^6 + B_3 S^4 + B_4 S^2 + B_5}{|(S+A)(S+B)(S^2+CS+D)(S^2+ES+F)|^2} \qquad \text{(B-3)}$$

The forms of Equations (B-1) and (B-2) must be transformed by a change of variable to the form of Equation (B-3). The program is BASIC language and is designed for the Hewlett-Packard 9830 calculator.

```
10 DISP "A,B,C,D,E,F";
20 INPUT A,B,C,D,E,F
22 DISP "BO-B5";
23 INPUT BO,B1,B2,B3,B4,B5
30 Z1=1
40 PRINT Z1
50 Z2=A+B+C+E
60 PRINT Z2
70 Z3=A*B+(A+B)*C+D+E*(A+B+C)+F
80 PRINT Z3
90 Z4=(A*B*C+(A+B)*D+E*(A*B+(A+B)*C+D)+F*(A+B+C))
```

```
100 PRINT Z4
110 Z5=(E*(A*B*C+(A+B)*D)+F*(A*B+(A+B)*C+D)+A*B*D)
120 PRINT Z5
130 Z6=A*B*D*E+F*(A*B*C+(A+B)*D)
140 PRINT Z6
150 Z7=F*A*B*D
160 PRINT Z7
170 H=Z1
171 I=Z2
172 J=Z3
173 K=Z4
175 L=Z5
177 M=Z6
178 N=Z7
180 A0=H
181 A1=I
182 A2=J
183 A3=K
184 A4=L
185 A5=M
186 A6=N
187 X=0
240 Z1=B0*(-A0*A3*A5*A6+A0*A4*(A5↑2)-(A1↑2)*A6↑2))
250 Z2=B0*(2*A1*A2*A5*A6+A1*A3*A4*A6)
260 Z3=B0*(-A1*(A4↑2)*A5-(A2↑2)*(A5↑2))
270 Z4=B0*(-A2*(A3↑2)*A6+A2*A3*A4*A5)
280 Z5=A0*B1*(-A1*A5*A6+A2*(A5↑2)+(A3↑2)*A6-A3*A4*A5)
290 Z6=A0*B2*(-A0*(A5↑2)-A1*A3*A6+A1*A4*A5)
300 Z7=A0*B3*(A0*A3*A5+(A1↑2)*A6-A1*A2*A5)
310 Z8=A0*B4*(A0*A1*A5-A0*(A3↑2)-(A1↑2)*A4+A1*A2*A3)
320 Z9=((A0*B5)/A6)*((A0↑2)*(A5↑2)+A0*A1*A3*A6)
330 Y1=((A0*B5)/A6)*(-2*A0*A1*A4*A5-A0*A2*A3*A5)
340 Y2=((A0*B5)/A6)/A6)*(A0*(A3↑2)*A4-(A1↑2)*A2*A6)
350 Y3=((A0*B5)/A6)*((A1↑2)*A4↑2)+A1*(A2↑2)*A5-A1*A2*A3*A4)
360 G1=(A0↑2)*(A5↑3)+3*A0*A1*A3*A5*A6-2*A0*A1*A4*(A5↑2)
370 G2=-A0*A2*A3*(A5↑2)-A0*(A3↑3)*A6+A0*(A3↑2)*A4*A5
380 G3=(A1↑3)*(A6↑2)-2*(A1↑2)*A2*A5*A6-(A1↑2)*A3*A4*A6+(A1↑2)
      *(A4↑2)*A5
390 G4=A1*(A2↑2)*(A5↑2)+A1*A2*(A3↑2)*A6-A1*A2*A3*A4*A5
400 M6=Z1+Z2+Z3+Z4+Z5+Z6+Z7+Z8+Z9+Y1+Y2+Y3
410 D6=G1+G2+G3+G4
415 IF X=1 THEN 500
420 I6=M6/(2*A0*D6)
430 PRINT I6
440 B0=B1
450 B1=B2
460 B2=B3
470 B3=B4
480 B4=B5
```

```
490 B5=0
491 X=1
495 GOTO 240
500 I7=-M6/(2*A0*D6)
510 PRINT I7
520 C0=(I6/I7)↑0.5
530 PRINT C0
540 END
```

The program will print the coefficients of S^6 to S^0 of the denominator. The integral values of I_0 and I_1 are then printed. Finally the value of η, the optimization factor from

$$\eta = \left(\frac{I_0}{I_2}\right)^{\frac{1}{2}} , \qquad \text{(B-4)}$$

is printed.

The method of integration is that of residues. This integral and others can be found in Reference 22.

APPENDIX C

The following program was used to calculate the time-response of the filters from the frequency-domain description of the filters. The input form is

$$H(S) = \frac{(MAG)(S^2+A)}{(S+B)(S+C)((S+D)^2+E^2)((S+F)^2+G^2)} \qquad \text{(C-1)}$$

other program inputs are the start and finish times and the incremental time step desired. The output consists of the value of time and the magnitude of the time-response at that time.

The program is

```
5 DISP "MAG =";
6 INPUT Q
10 DISP "START T";
15 INPUT J
16 DISP "FINISH T";
17 INPUT K
20 DISP "A,B,C,D,E,F,G";
30 INPUT A,B,C,D,E,F,G
40 DISP "TIME STEP";
50 INPUT T1
60 Z=0
65 Y=0
70 T=(T1*Z)+J
80 H=((B↑2+A)/((C-B)*((B-D)↑2+E↑2)*((B-F)↑2+G↑2)))*EXP(-B*T)
90 I=((C↑2+A)/((B-C)*((C-D)↑2+E↑2)*((C-F)↑2+G↑2)))*EXP(-C*T)
100 A1=((B-D)*(C-D)-E↑2)*((F-D)↑2+G↑2-E↑2)-(2*E↑2)*(F-D)*(C-2*D+B)
110 A3=((B-D)*(C-D)-E↑2)*2*E*(F-D)+E*(C-2*D+B)*((F-D)↑2+G↑2-E↑2)
120 B0=A1↑2+A3↑2
130 B1=A1*D-(A3/(2*E))*(D↑2+A-E↑2)
140 B2=(A1/(2*E))*(D↑2+A-E↑2)-D*A3
150 L1=EXP(-D*T)*COS(E*T)
160 L2=(-D/E)*EXP(-D*T)*SIN(E*T)
165 L3=(1/E)*EXP(-D*T)*SIN(E*T)*(2*B1*D+2*B2*E)/B0
170 A4=((B-F)*(C-F)-G↑2)*((D-F)↑2+E↑2-G↑2)-(2*G↑2)*(D-F)*(C-2*F+B)
```

```
180 A6=((B-F)*(C-F)-G↑2)*2*G*(D-F)+G*(C-2*F+B)*((D-F)↑2+E↑2-G↑2)
190 B5=A4↑2+A6↑2
200 B6=-A4*F-(A6/(2*G))*(F↑2+A-G↑2)
210 B7=(A4/(2*G))*(F↑2+A-G↑2)-F*AG
220 L4=EXP(-F*T)*C)S(G*T)
230 L5-(-F/G)*EXP(-F*T)*SIN(G*T)
235 L6=(1/G)*EXP(-F*T)*SIN(G*T)*(2*B6*F+2*B7*G)/B5
240 X=H+I+(2*B1/B0)*(L1+L2)+L3+(2*B6/B5)*(L4+L5)+L6
250 PRINT "T="T"MAG="Q*X
255 Y=Y+1
260 Z=Z+1
270 IF T<K THEN 70
280 IF T >= K THEN 300
300 END
```

The program is written for the Hewlett-Packard 9830 calculator.

APPENDIX D

The following two programs were used to calculate the integrals $\overline{V}$ and $\overline{V^2}$ respectively of Chapter VII. The program calculates the time response from the frequency domain equation. The program then integrates between two limits using the midpoint method. The limits are

$$T_{initial} = \text{START T} + \text{TIMESTEP}/2 \tag{D-1}$$

and

$$T_{final} = \text{FINISH T} + \text{TIMESTEP}/2 \tag{D-2}$$

The input form is

$$H(S) = \frac{(MAG)(S^2 + A)}{(S+B)(S+C)((S+D)^2+E^2)((S+F)^2+G^2)} \tag{D-3}$$

Time step is the incremental width of the time variable. The number of integral steps can be calculated from

$$\text{NO. OF STEPS} = \frac{\text{FINISH T-START T}}{\text{TIME STEP}} \tag{D-4}$$

The program for $\overline{V}$ is

```
5 DISP "MAG =";
6 INPUT Q
10 DISP "START T";
15 INPUT J
```

```
16 DISP "FINISH T";
17 INPUT K
20 DISP "A,B,C,D,E,F,G";
30 INPUT A,B,C,E,D,F,G
40 DISP "TIME STEP";
50 INPUT T1
60 Z=0
65 Y=0
66 N=0
70 T=(T1*Z)+J
80 H=((B↑2+A)/((C-B)*((B-D)↑2+E↑2)*((B-F)↑2+G↑2)))*EXP(-B*T)
90 T=((C↑2+A)/((B-C)*((C-D)↑2+E↑2)*((C-F)↑2+G↑2)))*EXP(-C*T)
100 A1=((B-D)*(C-D)-E↑2)*((F-D)↑2+G↑2-E↑2)-(2*E↑2)*(F-D)*(C-2*D+B)
110 A3=((B-D*(C-D)-E↑2)*2*E*(F-D)+E*(C-2*D+B)*((F-D)↑2+G↑2-E↑2)
120 B0=A1↑2+A3↑2
130 B1=-A1*D-(A3/(2*E))*D↑2+A-E↑2)
140 B2=(A1/(2*E))*(D↑2+A-E↑2)-D*A3
150 L1-EXP(-D*T)*COS(E*T)
160 L2=(-D/E)*EXP(-D*T)*SIN(E*T)
165 L3=(1/E)*EXP(-D*T)*SIN(E*T)*(2*B1*D+2*B2*E)/B0
170 A4=((B-F)*(C-F)-G↑2)*((D-F)↑2+E↑2-G↑2)-(2*G↑2)*(D-F)*(C-2*F+B)
180 A6=((B-F)*(C-F)-G↑2)*2*G*(D-F)+G*(C-2*F+B)*((D-F)↑2+E↑2-G↑2)
190 B5=A4↑2+A6↑2
200 B6=A4*F-(A6/(2*G))*(F↑2+A-G↑2)
210 B7=(A4/(2*G))*(F↑2+A-G↑2)-F*AG
220 L4=EXP(-F*T)*COS(G*T)
230 L5=(-F/G)*EXP(-F*T)*SIN(G*T)
235 L6=(1/G)*EXP(-F*T)*SIN(G*T)*(2*B6*F+2*B7*G)/B5
240 X=H+I+(2*B1/B0)*(L1+L2)+L3+(2*B6/B5)*(L4+L5)+L6
245 M=(Q*X)*(T1)
247 N=N+M
250 PRINT "T="1"MAG="(Q*X)"INT="N
255 Y=Y+1
260 Z=Z+1
270 IF T<K THEN 70
280 IF T >= K THEN 300
300 END
```

The program for $\overline{V^2}$ is

```
5 DISP "MAG =";
6 INPUT Q
10 DISP "START T";
15 INPUT J
16 DISP "FINISH T";
17 INPUT K
20 DISP "A,B,C,D,E,F,G";
```

```
30 INPUT A,B,C,D,E,F,G
40 DISP "TIME STEP";
50 INPUT T1
60 Z=0
65 Y=0
66 N=0
70 T=(T1*Z)+J
80 H=((B↑2+A)/((C-B)*((B-D)↑2+E↑2)*((B-F)↑2+G↑2)))*EXP(-B*T)
90 I=((C↑2+A)/((B-C)*((C-D)↑2+E↑2)*((C-F)↑2+G↑2)))*EXP(-C*T)
100 A1=((B-D)*(C-D)-E↑2)*((F-D)↑2+G↑2-E↑2)-(2*E↑2)*(F-D)*(C-2*D+B)
110 A3=((B-D)*(C-D)-E↑2)*2*E*(F-D)+E*(C-2*D+B)*((F-D)↑2+G↑2-E↑2)
120 B0=A1↑2+A3↑2
130 B1=-A1*D-(A3/(2*E))*(D↑2+A-E↑2)
140 B2=(A1/(2*E))*(D↑2+A-E↑2)-D*A3
150 L1=EXP(-D*T)COS(E*T)
160 L2=(-D/E)*EXP(-D*T)*SIN(E*T)
165 L3=(1/E)*EXP(-D*T)*SIN(E*T)*(2*B1*D+2*B2*E)/B0
170 A4=((B-F)*(C-F)-G↑2)*((D-F)↑2+E↑2-G↑2)-(2*G↑2)*(D-F)*(C-2*F+B)
180 A6=((B-F)*(C-F)-G↑2)*2*G*(D-F)+G*(C-2*F+B)*((D-F)↑2+E↑2-G↑2)
190 B5=A4↑2+A6↑2
200 B6=-A4*F-(A6/(2*G))*(F↑2+A-G↑2)
210 B7=(A4/(2*G))*F↑2+A-G↑2)-F*A6
220 L4=EXP(-F*T)*COS(G*T)
230 L5=(-F/G)*EXP(-F*T)*SIN(G*T)
235 L6=(1/G)*EXP(-F*T)*SIN(G*T)*(2*B6*F+2*B7*G)/B5
240 X=H+I+(2*B1/B0)*(L1+L2)+L3+(2*B6/B5)*(L4+L5)+L6
245 M=((Q*X)↑2)*(T1)
247 N=N+M
250 PRINT "T="T"MAG="(Q+X)↑2"INT="N
255 Y=Y+1
260 Z=Z+1
270 IF T<K THEN 70
280 IF T >= K THEN 300
300 END
```

The programs are written for the Hewlett-Packard 9830 calculator. The programs will print the time value, the magnitude of the functions at that time and the area under the curve up to that time.

VITA

Charles Lanier Britton, Jr., was born in Covington, Kentucky, on November 17, 1952. He attended secondary schools there, in Louisville, Kentucky, Kansas City, Missouri, Memphis, Tennessee, and Alcoa, Tennessee. He graduated from Alcoa High School in May, 1970. The following September, he entered The University of Tennessee, and in June, 1975, he received the Bachelor of Science degree in Electrical Engineering. In July of 1975, he began working as a consulting engineer for ORTEC, Inc., in Oak Ridge, Tennessee. In September of 1975 he began study towards a Master's degree.

The author is a member of Tau Beta Pi, Eta Kappa Nu, and Phi Kappa Phi. Mr. Britton is with the Hewlett-Packard Co. in Colorado Springs, Colorado.